Inorganic Chemistry

pubs.acs.org/IC Article

A One-Step Preparation of Tetradentate Ligands with Nitrogen and Phosphorus Donors by Reductive Amination and Representative Iron Complexes

Matthew V. Gradiski,[§] Ali Nemati Kharat,[§] Maegan S. E. Ong, Alan J. Lough, Samantha A. M. Smith, and Robert H. Morris*

Cite This: https://dx.doi.org/10.1021/acs.inorgchem.0c01535 Read Online

ACCESS | Metrics & More | Article Recommendations | Supporting Information

ABSTRACT: The synthesis and use of the first examples of unsymmetrical, mixed phosphine donor tripodal NPP_2' ligands $N(CH_2CH_2PR_2)_2(CH_2CH_2PPh_2)$ are presented. The ligands are synthesized via a convenient, one pot reductive amination using 2-(diphenylphosphino)ethylamine and various substituted phosphonium dimers in order to introduce mixed phosphine donors substituted with P/P′, those being Ph/Cy (**2**), Ph/^{i}Pr (**3**), Ph/^{i}Bu (**4**), Ph/*o*-Tol (**5**), and Ph/*p*-Tol (**6**). Additionally, we have developed the first known synthesis of a symmetrical tripodal NP_3 ligand $N(CH_2CH_2PiBu_2)_3$ using bench safe ammonium acetate as the lone nitrogen source (**7**). This new protocol eliminates the use of extremely dangerous nitrogen mustard reagents typically required to synthesize NP_3 ligands. Some of these tetradentate ligands and also P_2NN' ligands $N(CH_2$-*o*-$C_5H_4N)(CH_2CH_2PR_2)_2$ (P_2NN'-Cy, R = Cy; P_2NN'-Ph, R = Ph) prepared by reductive amination using 2-picolylamine are used in the synthesis and reactions of iron complexes. $FeCl_2(P_2NN'$-Cy) (**8**) undergoes single halide abstraction with $NaBPh_4$ to give the trigonal bipyramidal complex $[FeCl(P_2NN'$-Cy)$][BPh_4]$ (**9**). Upon exposure to CO(g), complex **9** readily coordinates CO giving $[FeCl(P_2NN'$-Cy)(CO)$][BPh_4]$ (**10**), and further treatment with an excess of $NaBH_4$ results in formation of the hydride complex $[Fe(H)(P_2NN'$-Cy)(CO)$][BPh_4]$ (**11**). Our previously reported complex $FeCl_2(P_2NN'$-Ph) undergoes double halide abstraction with $NaBPh_4$ in the presence of the coordinating solvent to give $[Fe(NCMe)_2(P_2NN'$-Ph)$][BPh_4]_2$ (**12**). Ligand **3** can be coordinated to $FeCl_2$, and upon sequential halide abstraction, treatment with $NaBH_4$, and exposure to an atmosphere of dinitrogen, the dinitrogen hydride complex $[Fe(H)(NPP_2'$-^{i}Pr)$(N_2)][BPh_4]$ (**13**) is isolated. Our symmetrical NP_3 ligand **7** can also be coordinated to $FeCl_2$ and, upon exposure to an atmosphere of CO(g), selectively forms $[FeCl(NP_3)(CO)][BPh_4]$ (**14**) after salt metathesis with $NaBPh_4$. Complex **14** can be treated with an excess of $NaBH_4$ to give the hydride complex $[Fe(H)(NP_3)(CO)][BPh_4]$ (**15**), which can further be deprotonated/reduced to the Fe(0) complex $Fe(NP_3)(CO)$ (**16**) upon treatment with an excess of KH.

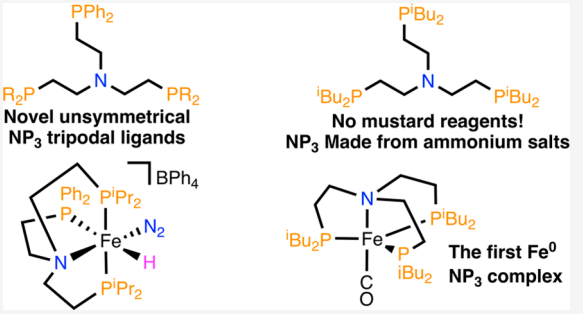

INTRODUCTION

This article reports a convenient, direct route to a variety of new tetradentate phosphine ligand architectures. Polyphosphines are one of the most commonly used classes of chelating ligands throughout inorganic coordination chemistry. Among them is the tridentate ligand triphos $MeC(CH_2PPh_2)_3$, and since its earliest reported synthesis by Hewertson and Watson in 1962,[1] triphos has shown widespread use as a ligand support on $RuCl_2$ for catalytic hydrogenation of olefins, aldehydes, ketones, and nitriles.[2] Triphos bearing *m*-xylyl substituents $MeC(CH_2P(m\text{-xyl})_2)_3$ has seen recent use on cobalt for the hydrogenation of carbonates to alcohols.[3] The related triphos ligand $N(CH_2PPh_2)_3$ (N-triphos) has a bridgehead nitrogen atom and is structurally very similar to triphos. Due to the constraints imposed by the methylene spacers between the nitrogen atom and phosphine donors, N-triphos chelates in a similar fashion to triphos as a tridentate ligand, and the nitrogen bridgehead does not coordinate to the metal center in, for example, complexes of molybdenum[4,5] and ruthenium.[6] In order for the ligand to adopt a tetradentate chelating mode which involves the nitrogen, more structural flexibility is needed. The introduction of ethylene spacers results in the tetradentate ligand, tris(2-diphenylphosphinoethyl)amine (NP_3). Sacconi pioneered the synthesis and coordination chemistry of this new class of ligands, and his group discovered various complexes and coordination geometries with chromi-

Received: May 25, 2020

https://dx.doi.org/10.1021/acs.inorgchem.0c01535
Inorg. Chem. XXXX, XXX, XXX−XXX

um,[7] cobalt,[8−11] and nickel.[8,12] It was shown that trigonal bipyramidal CoH(NP_3) complexes and tetrahedral $Ni^0(NP_3)$ react with formaldehyde to give, respectively, a cobalt hydrido carbonyl complex CoH(NP_3)(CO) and Ni^I formyl complex Ni(CHO)(NP_3) that readily decomposes to the Ni^0 carbonyl Ni(NP_3)(CO).[13] Additionally, rhodium and iridium(I) NP_3 supported complexes oxidatively add sp^2 C−H bonds.[14] Although the ligand prefers to coordinate in a tetradentate fashion, tridentate coordination is observed in the iridium(III) trihydride complex $IrH_3(\kappa^3$-P,P,P-$NP_3)$, which, upon treatment with HBF_4, undergoes oxidation to an iridium(V) tetrahydride and then subsequent reductive elimination of H_2 and coordination of the central nitrogen to produce the octahedral dihydride $IrH_2(\kappa^4$-N,P,P,P-$NP_3)$.[15] An interesting feature of iron(II) complexes bearing the NP_3 ligand or $NP^{i\text{-}Pr}_3$ ligand with isopropyl substituents at phosphorus[16] is their facile coordination of dinitrogen at ambient pressure.[17] Iron(0) complexes of the same NP_3 ligand can promote dinitrogen reduction to ammonia and hydrazine.[18] The NP_3 ligand has seen recent use with ruthenium for the catalytic dehydrogenation of formic acid,[19] as well as cobalt[20] and ruthenium[21] for the catalytic dehydrogenation of ammonia-borane. These two dehydrogenation processes have become more sought-after in recent years as hydrogen storage molecules become more important toward the development of sustainable fuels.[22−24] Nickel(II) NP_3 complexes are highly active for the catalytic hydrogenation of carbon dioxide to formate,[25] while ruthenium(0) NP_3 complexes are useful for dehydrogenative coupling of alcohols to esters.[26] P_4 tetraphos ligands have also been used for the synthesis of metal-hydride and dihydrogen complexes,[27,28] and recently, a tetradentate P_4N_2 ligand has been reported for the study of paramagnetic iron(I) hydrides.[29] Silicon has also been incorporated into the NP_3 framework, resulting in a tripodal amido-polyphosphine ligand.[30] An unsymmetrical NP_2P ligand with two chains linked by methylene spacers and one chain linked with an ethylene spacer has been reported with ruthenium for the hydrogenation of biobased carboxylic acids.[31] Increased flexibility can be achieved by lengthening the ethylene spacers to propylene in order to accommodate larger atoms like Mo(0).[32] Unsymmetrical tetradentate ligands have also been reported where one phosphorus donor is substituted for an additional nitrogen donor, resulting in an open-chain P_2N_2 framework if the nitrogen donors are geometrically equivalent, or a P_2NN' framework if they are not.[33] Chiral, open-chain P_2N_2 tetradentate ligands have been shown to be very useful ligands for the asymmetric transfer hydrogenation of polar bonds.[34−43] Chiral, macrocyclic P_2N_2 ligands have also been reported and are useful for similar asymmetric catalytic hydrogenations.[44−53]

Although tripodal NP_3 ligands have proven to be very versatile for a variety of applications, the nature of their synthesis continues to be a drawback in their use. Conventional synthesis of NP_3 ligands[8,16] requires the use of an extremely toxic and dangerous nitrogen mustard reagent tris(2-chloroethyl)amine (HN3). HN3 is a schedule 1 chemical weapon, the same classification given to sarin (*o*-isopropyl methylphosphonofluoridate) and bis(2-chloroethyl)sulfide, which is more commonly known as mustard gas. In addition, pyrophoric phosphides are required for the synthesis as well (Scheme 1). The need for S_N2 substitution with PR_2^- phosphides leads to an inability to vary phosphine substituents within the same ligand and is a highly limiting factor in the steric and electronic tunability of these ligands.

Scheme 1. Conventional Synthesis of NP_3 Ligands via Nitrogen Mustard and Phosphide Reagents

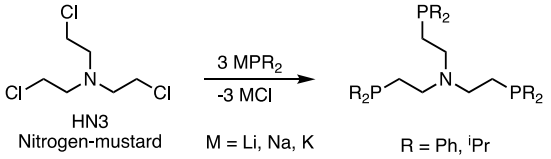

Recently, our group reported the synthesis of a variety of novel PNN′ and P_2NN' ligands via a one-step, one-pot reductive amination of primary amines with *in situ* generated primary phosphine acetaldehydes.[33] In addition to this recent study, our group has taken advantage of the use of phosphonium dimers to synthesize a wide variety of ligands and transition metal complexes.[37,39,54−59] In this work, we have expanded the use of our phosphonium dimer chemistry and report the first synthesis of a tetradentate tripodal NP_3 ligand via reductive amination using bench safe ammonium salts as the nitrogen source. Additionally, via the same synthetic route using the readily synthesized 2-(diphenylphosphino)-ethylamine as a precursor, we report the first synthesis of unsymmetrical mixed-phosphine donor NPP_2' tetradentate ligands. An overview of the ligands synthesized and used in this study is summarized and depicted in Scheme 2. The coordination chemistry of these ligands is explored with iron(II) resulting in the synthesis of NP_3 iron(II) carbonyl chlorides, carbonyl hydrides, and a mixed-donor NPP_2' dinitrogen hydride complex. Finally, the reactivity toward CO(g), hydride, and halide abstraction reagents of iron dichlorides supported by tetradentate P_2NN' ligands are investigated.

RESULTS AND DISCUSSION

Synthesis of Unsymmetrical NPP_2' and NP_3 Ligands. Our group has previously reported the synthesis of chiral P-NH-P′[55] and achiral PNN′ and P_2NN' ligands[33] via reductive amination of primary amines with phosphine aldehydes generated in situ via phosphonium dimers. The synthesis of novel unsymmetrical tripodal ligands NPP_2' adopts a similar synthetic strategy where the primary amine starting material is 2-(diphenylphosphino)ethylamine (**1**; Scheme 3). Compound **1** is commercially available in up to 95% purity; as an alternative, it is readily synthesized in 38% yield through S_N2 substitution of 2-bromoethylamine hydrobromide with an equivalent of diphenylphosphide in refluxing THF. We have found that before extracting the product with diethyl ether, stirring the residue in pentane removes almost all residual diphenylphosphine from the reaction mixture. By ^{31}P NMR (Figure S2), we observed only ∼2% diphenylphosphine, superior to commercial samples. Compound **1** is an important ligand in hydrogenation catalysis.[54,56,60−70]

For the reductive amination reaction, we use **1** and sodium trisacetoxyborohydride (STAB) with variously substituted phosphinoacetaldehydes that are generated from the reaction of the STAB base with its parent phosphonium dimers. This gives access to a variety of unsymmetrical NPP_2' tripodal ligands **2**−**6** (Scheme 3). After the reaction is complete, air-free aqueous workup to remove any residual sodium and borane salts is performed to isolate the ligands in fair to good yields (56−84%) and high purity. Ligands **2**−**6** have been characterized fully by ^1H and $^{31}P\{^1H\}$ NMR spectroscopy and DART mass spectrometry. The ligands all show a characteristic

https://dx.doi.org/10.1021/acs.inorgchem.0c01535
Inorg. Chem. XXXX, XXX, XXX−XXX

Scheme 2. Overview of the Synthesis of the Tetradentate Ligands of this Work

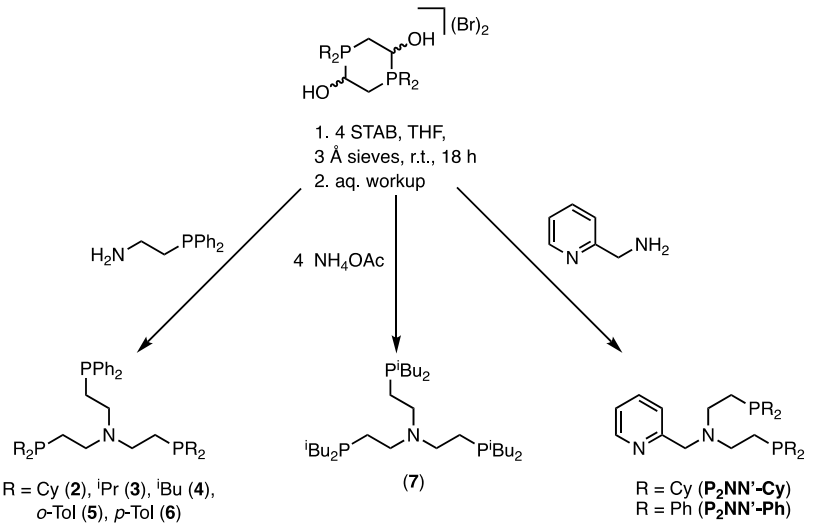

Scheme 3. Reductive Amination Synthesis of NPP_2' Ligands 2−6

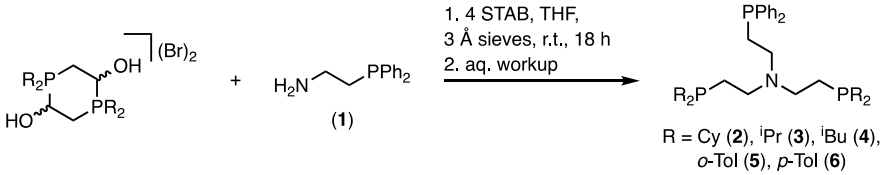

Scheme 4. Reductive Amination Synthesis of NP_3 Ligand 7

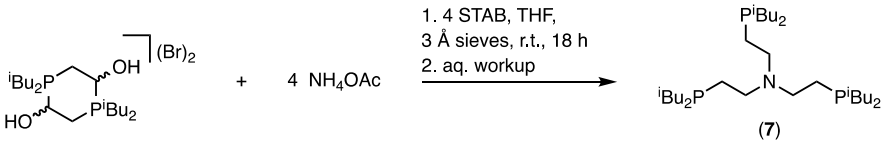

Scheme 5. Synthesis of P_2NN'-Cy Complexes 8 and 9

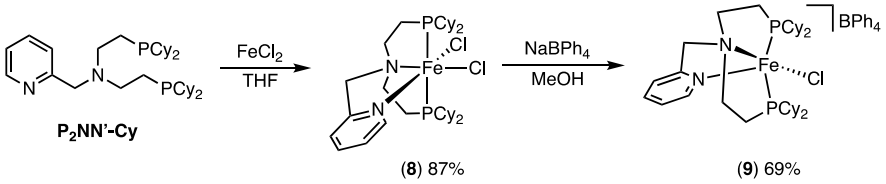

resonance in their $^{31}P\{^1H\}$ spectrum around −20 ppm corresponding to the phenyl substituted arm and a second resonance ranging from 1.8 (R = ^{i}Pr) to −41 ppm (R = ^{i}Bu, *o*Tol).

Symmetrical NP_3 tetradentate ligands can also be synthesized using ammonium salts as the lone nitrogen source. During optimization of the reaction conditions (SI Table S1), it was observed that the use of NH_4Cl, even in 20-fold excess, yielded only ∼6% of the desired NP_3 product. Upon switching to NH_4OAc, a considerable increase in the yield to 63% was achieved with 1.5 equiv of the salt. The optimum amount was 4 equiv of NH_4OAc, producing the ligand in 71% yield; further increases in the amount of salt did not significantly improve the yield. Since NP_3 ligands with phenyl[12] and isopropyl[16] substituents at phosphorus have previously been reported, we opted to use an isobutyl-substituted phosphonium dimer in order to create a novel NP_3 ligand. A similar synthetic strategy used in the synthesis of ligands **2−6** was adopted: one equivalent of phosphonium dimer and four equivalents of NH_4OAc and STAB in THF reacted to give the tripodal NP_3 ligand **7** in 91% isolated yield after aqueous workup (Scheme 4). The ligand displays a sharp singlet at −41.6 ppm in the $^{31}P\{^1H\}$ NMR spectrum owing to the three equivalent phosphorus atoms; ^1H NMR spectroscopy and mass spectrometry with DART detection confirmed the structure.

Synthesis and Reactivity of P_2NN' Supported Iron Complexes. Recently, our lab reported the synthesis of tetradentate P_2NN'-Cy and P_2NN'-Ph ligands and an iron complex $FeCl_2(P_2NN'$-Ph).[33] Here, we report the synthesis of iron complexes where the ligand bears cyclohexyl substituents at phosphorus. One equivalent of the P_2NN'-Cy ligand reacts with $FeCl_2$ in THF to give the octahedral complex $FeCl_2(P_2NN'$-Cy) (**8**; Scheme 5).

Single crystal X-ray diffraction (XRD) of complex **8** confirms a distorted octahedral geometry with *trans* phosphorus donors while the tertiary amine, pyridine, and two chloride ligands all

https://dx.doi.org/10.1021/acs.inorgchem.0c01535
Inorg. Chem. XXXX, XXX, XXX−XXX

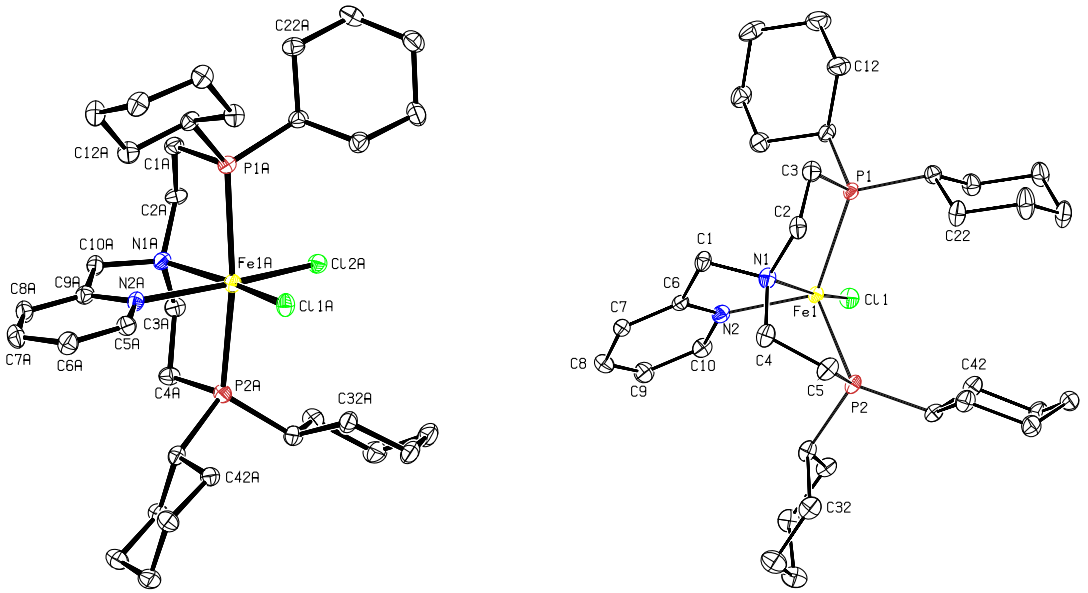

Figure 1. X-ray structure of **8** (left) and **9** (right). Ellipsoids are shown at 30% probability. Hydrogen atoms and tetraphenylborate anion have been omitted for clarity. There were two independent molecules in the asymmetric unit for **8**. Molecule A is shown here, and molecule B is provided in Figure S16. Selected bond lengths (Å) and angles (deg) for **8**: Fe(1A)−N(2A) 2.219(3), Fe(1A)−Cl(1A) 2.3452(12), Fe(1A)−N(1A) 2.393(3), Fe(1A)−Cl(2A) 2.4723(12), Fe(1A)−P(1A) 2.5192(12), Fe(1A)−P(2A) 2.5501(13); N(2A)−Fe(1A)−Cl(1A) 96.19(10), N(2A)−Fe(1A)−N(1A) 74.03(12), Cl(1A)−Fe(1A)−N(1A) 169.93(9), N(2A)−Fe(1A)−Cl(2A) 158.36(10), P(1A)−Fe(1A)−P(2A) 159.62(5); for **9**: Fe(1)−N(2) 2.1161(19), Fe(1)−Cl(1) 2.2825(7), Fe(1)−P(1) 2.4275(7), Fe(1)−P(2) 2.4629(7); N(1)−Fe(1)−Cl(1) 170.31(5), N(2)−Fe(1)−Cl(1) 101.05(6), N(2)−Fe(1)−P(1) 120.99(5), Cl(1)−Fe(1)−P(1) 98.04(3), N(2)−Fe(1)−P(2) 102.76(6), Cl(1)−Fe(1)−P(2) 111.12(3), P(1)−Fe(1)−P(2) 120.93(3).

Scheme 6. Synthesis of P_2NN'-Cy Complexes 10 and 11

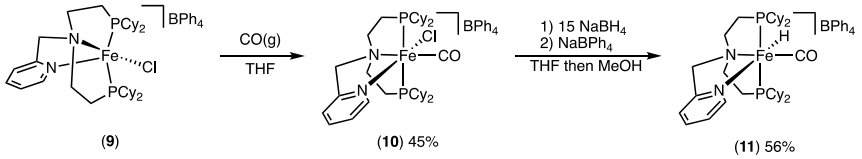

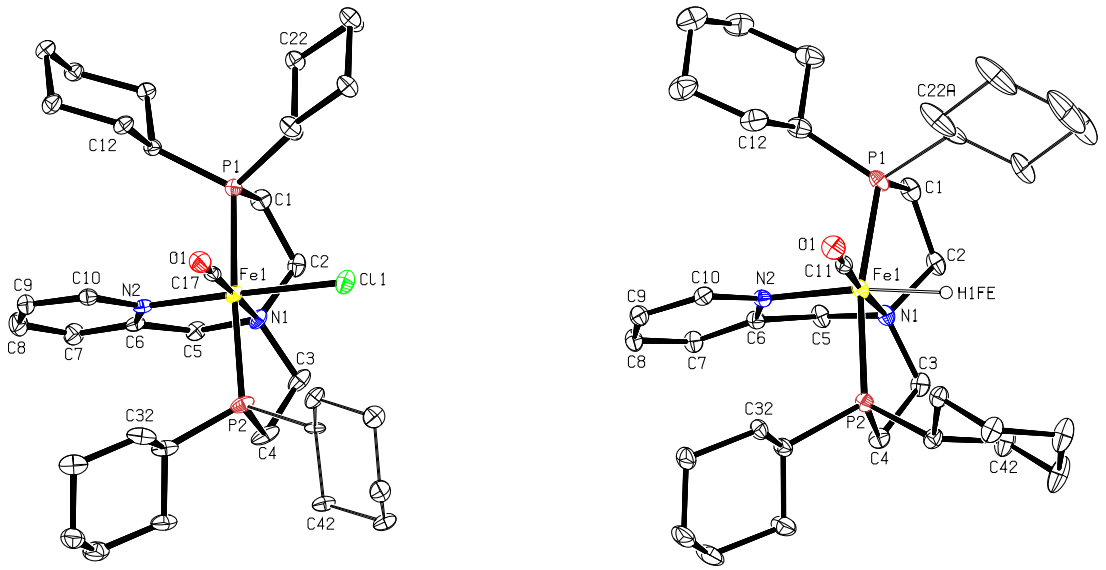

Figure 2. Structure of the cations of **10** (left) and **11** (right). Ellipsoids are shown at 30% probability. Hydrogen atoms (except hydride ligand) and tetraphenylborate anions have been omitted for clarity. Selected bond lengths (Å) and angles (deg) for **10**: Fe(1)−C(17) 1.796(3), Fe(1)−N(2) 1.969(2), Fe(1)−N(1) 2.086(2), Fe(1)−P(2) 2.2886(9), Fe(1)−P(1) 2.2953(8), Fe(1)−Cl(1) 2.3222(8); C(17)−Fe(1)−N(1) 179.11(11), N(2)−Fe(1)−N(1) 83.82(9), N(2)−Fe(1)−P(1) 90.48(7), P(2)−Fe(1)−P(1) 170.36(3); for **11**: Fe(1)−C(11) 1.720(3), Fe(1)−N(2) 2.004(3), Fe(1)−N(1) 2.097(3), Fe(1)−P(1) 2.2021(9), Fe(1)−P(2) 2.2227(9), Fe(1)−H(1FE) 1.67(5); C(11)−Fe(1)−N(1) 176.53(12), N(2)−Fe(1)−N(1) 83.06(10), N(2)−Fe(1)−P(1) 98.14(8), P(1)−Fe(1)−P(2) 167.16(4).

https://dx.doi.org/10.1021/acs.inorgchem.0c01535
Inorg. Chem. XXXX, XXX, XXX−XXX

lie in a plane (Figure 1). Complex **8** is paramagnetic as evidenced by its broad and paramagnetically shifted ^{1}H NMR spectrum (Figure S15). The solution magnetic susceptibility is 5.49 μ_B as measured via Evan's method and is consistent with a high spin Fe(II) center with four unpaired electrons. Cyclohexyl substituents do not have a significant impact on the P−Fe−P bond angle of 159.62(5)°, which is similar to 160.57(3)° in $FeCl_2(P_2NN'$-Ph); however, one of the Fe−P bonds lengths shortens from 2.6110(9) Å in $FeCl_2(P_2NN'$-Ph) to 2.550(1) Å in **8** owing to the stronger phosphine donor with alkyl substituents.

Treatment of **8** with one equivalent of $NaBPh_4$ in methanol cleanly yields the halide abstracted, five-coordinate cationic complex $[FeCl(P_2NN'$-Cy)$][BPh_4]$ (**9**; Scheme 5). Single crystal XRD of **9** (Figure 1) shows a distorted trigonal bipyramidal geometry with a τ_5 geometry index value of 0.82 with amine nitrogen approximately *trans* to chloride (Cl(1A)−Fe(1A)−N(1A) 169.93(9)°) and a P−Fe−P bond angle of 120.93(3)°. There are five five-coordinate iron complexes Fe(N-donor)$_2$(P-donor)$_2$Cl in the Cambridge Structural Database (CSD), but they are all square pyramidal and neutral.[71−75] There are two structures of trigonal bipyramidal $[FeCl(P(CH_2CH_2PR_2)_3)]^+$ in the literature: R = Cy[76] and R = iPr.[77] Surprisingly, the normally higher *trans* influence of phosphorus over nitrogen is not seen in these complexes since shorter Fe−Cl bond lengths are found for the PP_3 complexes with R = Cy (2.235(4) Å) and R = iPr (2.2371(3)) versus the P_2NN'-Cy complex **9** (2.2825(7)).

Complex **9** is readily soluble in dichloromethane; however it is practically insoluble in chloroform, possibly due to the cationic nature of the complex. Complex **9** has a solution magnetic susceptibility of 5.31 μ_B owing to a high spin Fe(II) center with four unpaired electrons. As in the case with other paramagnetic transition metal phosphine complexes, **8** and **9** are ^{31}P NMR silent.

Upon exposure of **9** to CO(g), a significant color change from light yellow to dark green is observed, suggesting coordination of CO to the empty coordination site (Scheme 6).

Single crystal XRD of the newly isolated yellow-green compound confirms the formation of the cationic octahedral complex $[FeCl(P_2NN'$-Cy)(CO)$][BPh_4]$ (**10**) with carbonyl *trans* to the apical nitrogen and the two bulky PCy_2 groups in *trans* positions (Figure 2). The FT-IR spectrum of **10** also reveals a sharp CO stretch at 1960 cm^{-1}. Complex **10** has less distortion to its octahedral geometry than **8** as observed by a P−Fe−P bond angle of 170.36(3)°, and it has significantly shorter Fe−P bond lengths of 2.2886(9) and 2.2953(8) Å than **8**. Short Fe−P bond lengths coincide with a low spin Fe(II) center, and the diamagnetic nature of **10** is confirmed via ^{31}P{^{1}H} NMR spectroscopy where a sharp singlet at 66.5 ppm is observed in the ^{31}P{^{1}H} NMR spectrum. The five other Fe(CO)Cl(N-donor)$_2$(P-donor)$_2$ complexes with tetradentate ligand complexes in the CSD have linear PNNP ligands with carbonyl *trans* to chloride and are also diamagnetic.[36,78−80]

The addition of a large excess (15 equiv) of $NaBH_4$ to complex **10** in THF gives access to the hydride complex $[Fe(H)(P_2NN'$-Cy)(CO)$][BPh_4]$ (**11**; Scheme 6). Single crystal XRD confirms the substitution of the chloride ligand with a hydride (Figure 2). While there is only one other structurally characterized tetradentate iron complex with the Fe(CO)(H)(P)$_2$(N)$_2$ donor set,[78] there are a variety of structures of hydridocarbonyl complexes with PNP pincer ligands.[81−85] All but one[85] of these structures have the common features like those in **11** of a hydride trans to nitrogen and carbonyl trans to nitrogen. The resonance of the hydride is observed in the ^{1}H NMR spectrum as a triplet shifted significantly upfield to −18.75 ppm with a $^2J_{HP}$ of 53.0 Hz. A change in the ^{31}P{^{1}H} NMR is also observed most notably by the splitting of the resonance into a doublet owing to coupling with the hydride ligand ($^2J_{PH}$ = 14.7 Hz) along with a downfield shift from the chloride complex to 82.5 ppm. The CO stretch of **11** also experiences a shift of ∼60 cm^{-1} to 1900 cm^{-1} in the FT-IR spectrum. Usually, monocationic iron complexes with hydride trans to pyridine are expected to have an Fe−H stretch near 1940 cm^{-1}, and there is a weak absorption in this region.[86]

The poor solubility of the reported complex $FeCl_2(P_2NN'$-Ph) in MeOH did not allow a similar halide abstraction reaction to that of Scheme 5. Instead, we now find that the use of acetonitrile allows a rapid double chloride substitution by acetonitrile to occur to give the octahedral dication $[Fe(NCMe)_2(P_2NN'$-Ph)$][BPh_4]_2$ (**12**; Scheme 7). The Fe−P

Scheme 7. Synthesis of Dicationic Complex 12

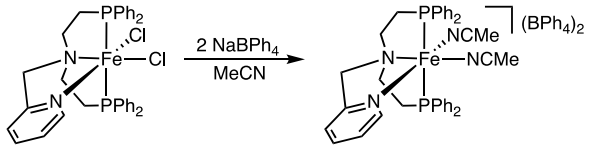

$FeCl_2(P_2NN'$-Ph) **(12)** 82%

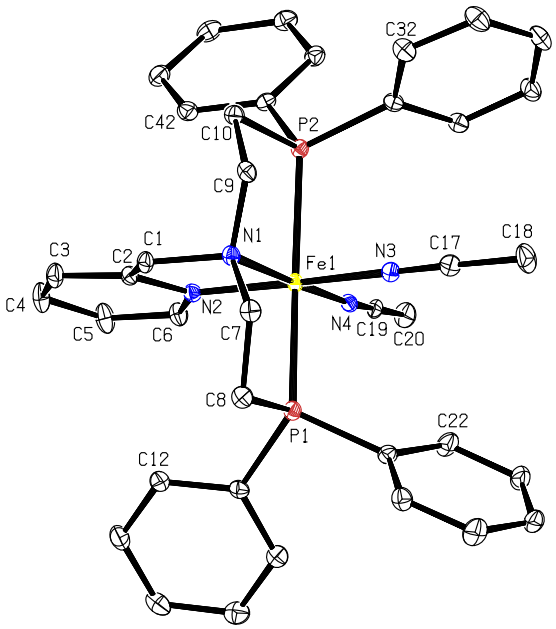

Figure 3. X-ray structure of the dication of **12**. Ellipsoids are shown at 30% probability. Hydrogen atoms and tetraphenylborate anions have been omitted for clarity. Selected bond lengths (Å) and angles (deg): Fe(1)−N(3) 1.9028(19), Fe(1)−N(4) 1.9325(19), Fe(1)−N(2) 1.9661(19), Fe(1)−N(1) 2.0597(19), Fe(1)−P(1) 2.2811(7), Fe(1)−P(2) 2.2859(7); P(1)−Fe(1)−P(2) 169.58(3), N(1)−Fe(1)−P(2) 85.99(6), N(3)−Fe(1)−N(2) 175.80(8), N(3)−Fe(1)−N(4) 91.80(8), N(2)−Fe(1)−N(1) 83.92(8).

https://dx.doi.org/10.1021/acs.inorgchem.0c01535
Inorg. Chem. XXXX, XXX, XXX−XXX

Scheme 8. Synthesis of the Dinitrogen Complex 13

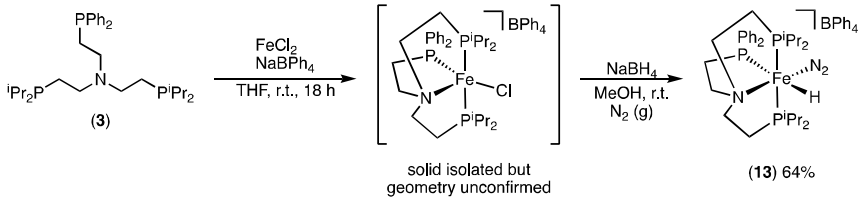

bond lengths in **12** confirmed by single crystal XRD (Figure 3) of 2.2811(7) and 2.2859(7) Å, respectively, are very similar to those in **10**, which is also low spin. Dicationic iron complexes $[FeN_4P_2]^{2+}$ with at least two MeCN ligands are common with 44 structures in the CSD. The complex is completely insoluble in nearly all common organic and chlorinated solvents except acetonitrile. **12** displays a sharp singlet in its $^{31}P\{^1H\}$ NMR spectrum at 56.4 ppm, further confirming its diamagnetic nature. Replacement of the chloride ligands appears to occur stepwise, albeit very quickly. After the addition of $NaBPh_4$, the mixture experiences a color change to dark green, which persists for only a few seconds before changing to orange and forming the isolated product. The driving force for double halide abstraction may be the preference for formation of a diamagnetic low spin six-coordinate complex as opposed to a paramagnetic five-coordinate complex like **9**.

Synthesis and Reactivity of NPP_2' and NP_3 Tripodal Iron Complexes. In order to demonstrate the utility of our mixed phosphine donor NPP_2' ligands, we synthesized a dinitrogen hydride complex similar to the two complexes $[Fe(H)(N(CH_2CH_2PR_2)_3(N_2)]^+$, R = Ph and R = ^{i}Pr, that have previously been reported in the literature.[16,17] We opted to use ligand **3** with mixed phenyl and isopropyl phosphine donors in order to observe the effect of asymmetry on the complex structure and reactivity. Ligand **3** was reacted with one equivalent of $FeCl_2$ and $NaBPh_4$ in THF to give a pale yellow solid. Suitable crystals for XRD could not be obtained. Nonetheless, its silent $^{31}P\{^1H\}$ NMR spectrum supports the formation of a paramagnetic complex $[FeCl(NPP_2'\text{-}^iPr)]^+$, by analogy to the reaction in Scheme 5. The isolated product from this reaction was then treated with six equivalents of $NaBH_4$ at −30 °C under an argon atmosphere resulting in an orange solution (Scheme 8).

Upon redissolving the residue of this reaction in benzene and exposing it to a nitrogen atmosphere by way of the glovebox, a color change to green was observed. Single crystal XRD (Figure 4) confirmed the uptake of dinitrogen by the iron complex as well as the presence of a hydride, giving $[Fe(H)(NPP_2'\text{-}^iPr)(N_2)][BPh_4]$ (**13**). This octahedral complex has the dinitrogen ligand *trans* to the apical N and the bulky P^iPr_2 groups *trans* to each other. The N_2 ligand in the other known complexes $[Fe(H)(NP_3\text{-}^iPr)(N_2)][PF_6]$ and $[Fe(H)(NP_3\text{-Ph})(N_2)][BPh_4]$ is also positioned *trans* to the bridgehead nitrogen. The N−N distance of **13** measured at 1.124(2) Å is slightly longer than those in NP_3-^{i}Pr and NP_3-Ph complexes of 1.114(4)[16] and 1.102(12)[18] Å, respectively. The complex is diamagnetic as evidenced by the two resonances observed in the $^{31}P\{^1H\}$ NMR at 74.5 and 47.6 ppm, respectively. The hydride resonance in the ^{1}H NMR spectrum at −9.30 ppm is a doublet of triplets with the *trans* $^2J_{HP}$ = 62.6 Hz coupling with the PPh_2 P nucleus slightly larger than the *cis* coupling of 44.6 Hz with the P^iPr_2 P nuclei. Both the metal-hydride and dinitrogen stretches are observed in the FT-IR

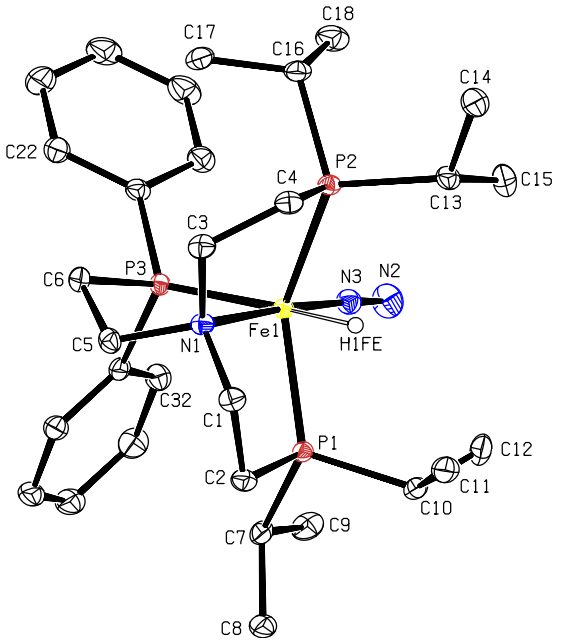

Figure 4. Structure of the cation of **13**. Ellipsoids are shown at 30% probability. Hydrogen atoms (except the hydride ligand) and the tetraphenylborate anion have been omitted for clarity. Selected bond lengths (Å) and angles (deg): Fe(1)−N(3) 1.7901(14), Fe(1)−N(1) 2.1106(12), Fe(1)−P(1) 2.2406(4), Fe(1)−P(3) 2.2478(4), Fe(1)−P(2) 2.2532(4), Fe(1)−H(1FE) 1.441(19), N(2)−N(3) 1.124(2); N(3)−Fe(1)−N(1) 176.12(6), N(1)−Fe(1)−P(1) 85.26(4), N(3)−Fe(1)−P(2) 96.96(5), P(1)−Fe(1)−P(2) 140.459(17).

spectrum at 1909 and 2080 cm^{-1}, respectively. The $\nu(N_2)$ of 2080 cm^{-1} is lower than that of $[Fe(H)(NP_3\text{-Ph})(N_2)][BPh_4]$ and $[Fe(H)(NP_3\text{-}^iPr)(N_2)][PF_6]$, which have a $\nu(N_2)$ of 2090 and 2087 cm^{-1}, respectively. In complex **13**, the Fe−N distance trans to the N_2 ligand of 2.111(1) Å is the same as the NP_3-Ph complex of 2.119(8) Å and shorter than that in the NP_3-^{i}Pr complex of 2.147(3) Å. Additionally, the Fe−P distance trans to the hydride ligand is shorter in **13** at 2.2478(4) Å than in either symmetrical complex: 2.257(4) Å for NP_3-Ph and 2.286(1) Å for NP_3-^{i}Pr. Therefore, the unsymmetrical ligand binds stronger and results in more donation into the metal center as well as into the N_2 π^* orbital, giving rise to a lower $\nu(N_2)$.

Complex **13** is extremely sensitive toward air and moisture and decomposes in the presence of dichloromethane vapor. Reactions attempting to synthesize carbonyl compounds were carried out on starting complexes bearing unsymmetrical NPP_2' ligands of the assumed structure $[Fe(Cl)(NPP_2')][Cl]$ of Scheme 8. Upon exposure to CO(g) at liquid nitrogen temperature, the solution first turned dark blue and then upon slow warming turned brown. Unfortunately, we could not characterize the mixture that was produced.

https://dx.doi.org/10.1021/acs.inorgchem.0c01535
Inorg. Chem. XXXX, XXX, XXX−XXX

Scheme 9. Synthesis of Complexes 14 and 15

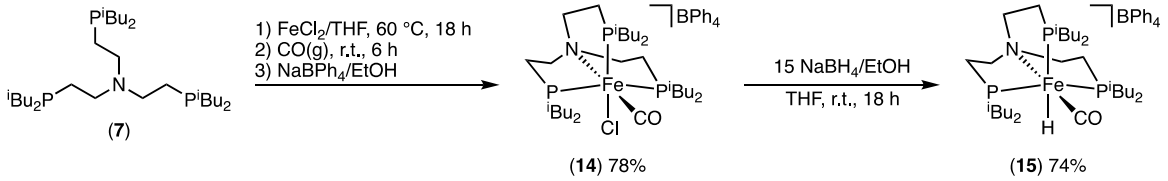

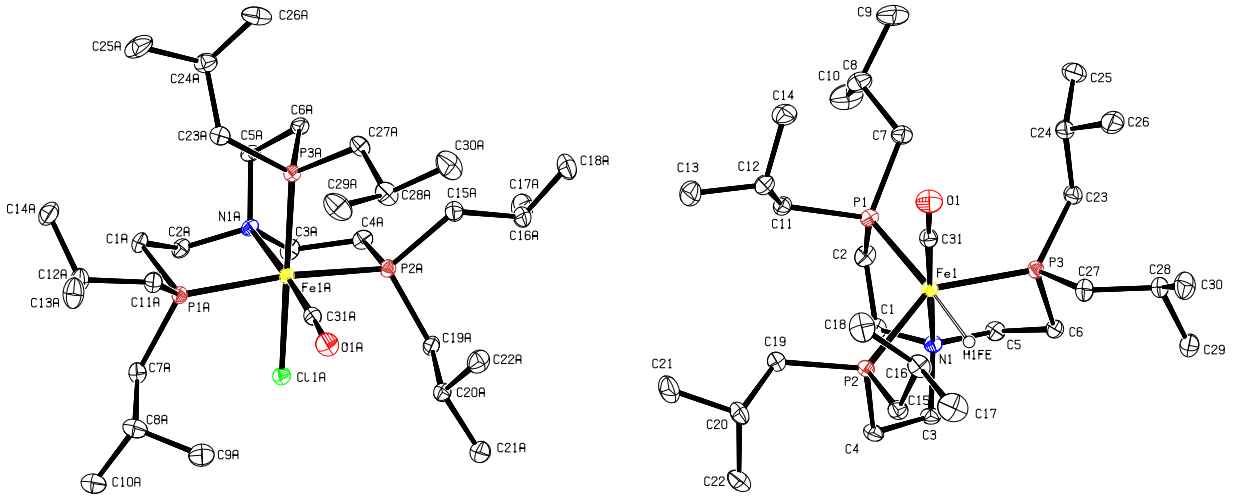

Figure 5. Structures of the cations of **14** (left) and **15** (right). Ellipsoids are shown at 30% probability. Hydrogen atoms (except the hydride ligand) and tetraphenylborate anions have been omitted for clarity. There were two independent ion pairs in the asymmetric unit for **14**. The cation of A is shown here, and B is shown in the Supporting Information (Figure S32). Selected bond lengths (Å) and angles (deg) for **14**: Fe(1A)−C(31A) 1.737(5), Fe(1A)−N(1A) 2.147(4), Fe(1A)−P(3A) 2.2618(12), Fe(1A)−P(1A) 2.2867(13), Fe(1A)−P(2A) 2.3250(13), Fe(1A)−Cl(1A) 2.3526(12); C(31A)−Fe(1A)−N(1A) 177.2(2), C(31A)−Fe(1A)−P(3A) 96.82(16), N(1A)−Fe(1A)−P(1A) 86.18(12), P(1A)−Fe(1A)−P(2A) 165.31(5); for **15**: Fe(1)−C(31) 1.7303(17), Fe(1)−N(1) 2.1093(14), Fe(1)−P(3) 2.2136(5), Fe(1)−P(2) 2.2192(5), Fe(1)−P(1) 2.2200(5), Fe(1)−H(1FE) 1.460(19); C(31)−Fe(1)−N(1) 175.75(7), C(31)−Fe(1)−P(3) 91.39(6), P(3)−Fe(1)−P(2) 138.617(19), N(1)−Fe(1)−P(1) 85.88(4).

We are interested in estimating the acidity of transition metal hydride complexes[87] and found that iron(II) carbonyl phosphine complexes show a linear increase in pK_a in THF as carbonyl ligands are replaced by trialkyl phosphine donors.[88] The carbonyl hydride $[FeH(CO)(NP_3)]^+$ prepared using our NP_3 ligand **7** was predicted using the LAC method[87] to be a weak acid (pK_a^{LAC} 21). This complex was prepared according to Scheme 9. First **7** and $FeCl_2$ are heated in THF, presumably forming an octahedral dichloride complex that was not isolated. Exposure of the reaction mixture to an atmosphere of CO(g) results in a color change from beige to brown with the selective substitution of chloride for CO. Salt metathesis with $NaBPh_4$ in alcohol solvent allows for the precipitation of $[FeCl(NP_3)(CO)][BPh_4]$ (**14**) as the tetraphenylborate salt.

XRD of a crystal of **14** (Figure 5) confirms the octahedral geometry where the NP_3 ligand coordinates in a tetradentate fashion along with the CO ligand *trans* to the nitrogen. The complex is diamagnetic, and two resonances are observed in the $^{31}P\{^1H\}$ NMR spectrum corresponding to the two chemically inequivalent phosphorus environments. A doublet corresponding to the *trans* phosphine donors is observed at 49.5 ppm with $^2J_{PP}$ = 42.5 Hz, and a triplet corresponding to the phosphine donor trans to chloride is observed at 69.8 ppm with the same $^2J_{PP}$. A strong CO stretch is observed in the FT-IR spectrum centered at 1940 cm^{-1}. The treatment of **14** with an excess of sodium borohydride results in the substitution of the chloride ligand for a hydride to give the complex $[Fe(H)(NP_3)(CO)][BPh_4]$ (**15**; Scheme 9). XRD of a single crystal of **15** (Figure 5) confirms the presence of a hydride with the CO ligand remaining *trans* to the nitrogen as in compounds **10** and **11**. Two similar complexes $[Fe(H)(CO)(N(CH_2CH_2PR_2)_3)]^+$ have been structurally characterized with R = ^{i}Pr[16] and R = Ph.[18] The hydride resonance of **15** is seen in the ^1H NMR spectrum at −11.2 ppm as a doublet of triplets with the *trans* $^2J_{HP}$ coupling of 68 Hz being larger than the *cis* $^2J_{HP}$ coupling of 34 Hz. The $^{31}P\{^1H\}$ NMR spectrum is an A_2B pattern with *cis* $^2J_{PP}$ of 20 Hz. A shift in the CO stretch is also observed with **15** in the FT-IR to 1903 cm^{-1}. Complex **15** is significantly more stable (less reducing) than the dinitrogen complex **13**, and NMR spectroscopy can be conducted in $CDCl_3$; however it is still sensitive to air and moisture. Treatment of complex **15** with an excess of the strong base KH at room temperature in THF results in the slow deprotonation of the hydride, a two electron reductive elimination process, to give trigonal bipyramidal $Fe^0(NP_3)(CO)$ (**16**) accompanied by the loss of H_2 and precipitation of $KBPh_4$ from solution (Scheme 10).

Single crystal XRD (Figure 6) of **16** confirms the trigonal bipyramidal geometry which is nearly ideal with a calculated τ_5 value of 0.96. Reduction to Fe(0) is also evidenced by the Fe−P bond lengths which are significantly shorter in **16** than in **15** by ∼0.1 Å and are measured at 2.1514(4) and 2.1633(4) Å, respectively. The shortening is thought to be a result of less interligand repulsion around the equatorial plane of the trigonal bipyramid compared to that in the octahedral complex **15**.

https://dx.doi.org/10.1021/acs.inorgchem.0c01535
Inorg. Chem. XXXX, XXX, XXX−XXX

Scheme 10. Deprotonation/Reduction of 15 to Complex 16 with KH

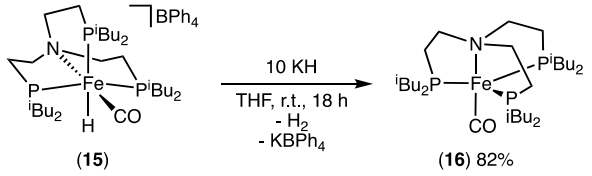

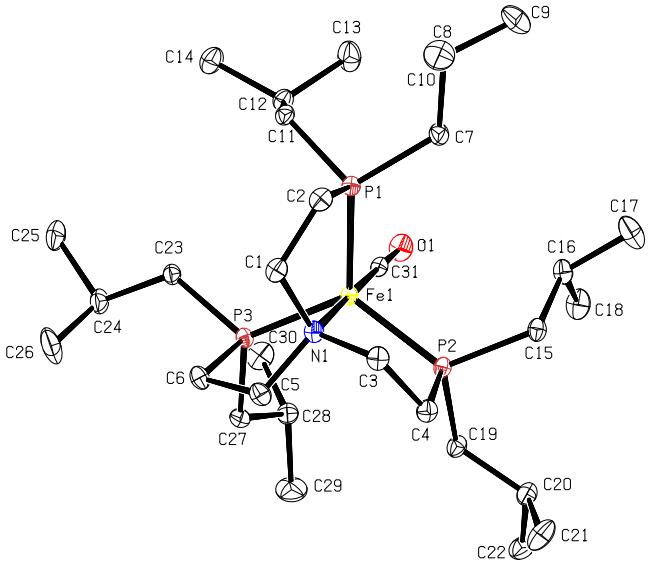

Figure 6. Molecular structure of **16**. Ellipsoids are shown at 30% probability. Hydrogen atoms have been omitted for clarity. Selected bond lengths (Å) and angles (deg): Fe(1)−C(31) 1.7171(15), Fe(1)−N(1) 2.1325(13), Fe(1)−P(2) 2.1514(4), Fe(1)−P(1) 2.1633(4), Fe(1)−P(3) 2.1646(4); C(31)−Fe(1)−N(1) 179.04(6), N(1)−Fe(1)−P(1) 85.78(4), P(2)−Fe(1)−P(1) 119.321(17), P(2)−Fe(1)−P(3) 121.161(17).

Additional evidence for the reduction can be seen in the FT-IR spectrum of **16** where the CO stretch at 1808 cm^{-1} is significantly lower than that of the Fe(II) complex **15**. This significant change in the CO stretch is also consistent with the C−O bond lengths in **15** and **16**. Complex **15** with a higher ν(CO) has a shorter C−O bond length of 1.160(2) Å, whereas complex **16**, with a lower ν(CO), has a slightly longer one of 1.180(2) Å. While no NP_3 hydride complexes of iron have been deprotonated in this way, the related PP_3 complex $[FeH(CO)(P(CH_2CH_2PMe_2)_3]^+$ has been treated with KO^{t}Bu in THF to produce Fe(CO)(PP_3) with ν(CO) 1855 cm^{-1}.[89]

CONCLUSION

A variety of novel unsymmetrical mixed phosphine donor NPP_2' tripodal ligands (**2**−**6**) have been synthesized via reductive amination of tertiary phosphine acetaldehydes with 2-aminoethyldiphenylphosphine. An improvement in the synthesis of the latter compound, an important precursor to ligands and catalysts, has also been described. Additionally, a symmetrical NP_3 tripodal ligand (**7**) can be synthesized via the same methods using ammonium salts as the nitrogen source, eliminating the need for dangerous reagents. The previously reported ligand P_2NN'-Cy is now used for coordination chemistry. These tetradentate ligands (collectively labeled L) provide a direct route to Fe(II) complexes of the types $FeCl_2L$ (**8**), $[FeCl(L)]^+$ (**9**), $[Fe(MeCN)_2L]^{2+}$ (**12**), $[FeCl(CO)L]^+$ (**10**, **14**), $[FeH(N_2)L]^+$ (**13**), and $[FeH(CO)L]^+$ (**11**, **15**). Evidence is provided that the mixed donor ligand NPP_2'-^{i}Pr (**3**) in the complex $[FeH(N_2)(NPP_2'$-^{i}Pr$)]^+$ (**13**) is more tightly bound than either of the symmetrical ligands NP_3-Ph or NP'_3-^{i}Pr, resulting in the lowest N_2 stretch of the three dinitrogen complexes. The hydride complex $[FeH(CO)(NP_3)]BPh_4$ (**15**) is a very weak acid but undergoes deprotonation/reduction by the strong base KH to produce the Fe(0) complex Fe(CO)(NP_3) (**16**). Notable features of the iron complexes include the first structures of a trigonal bipyramidal five coordinate $FeClN_2P_2^+$ donor set in **9** with an unexpectedly long Fe−Cl bond, a rare hydridocarbonyl complex with the Fe(CO)(H)$(P)_2(N)_2$ donor set in **11**, and the first trigonal bipyramidal structure of the type $Fe^0(NP_3)$-(CO) in **16**.

EXPERIMENTAL SECTION

General Considerations. All experimental procedures and manipulations were conducted under a dinitrogen or argon atmosphere using standard Schlenk-line and glovebox procedures unless otherwise stated. All solvents were degassed and dried using standard procedures prior to all procedures. 2-Bromoethylamine hydrobromide, ammonium acetate, and sodium trisacetoxyborohydride (STAB) were purchased from Sigma-Aldrich and used without further purification. Anhydrous $FeCl_2$ (99.5%) was purchased from Alfa Aesar and used without further purification. Phosphonium dimers were synthesized according to the literature procedure.[90] Bis[*N*-(2-(dicyclohexylphosphino)ethyl)-*N*-(pyridin-2-ylmethyl)amine (P_2NN'-Cy) and $FeCl_2(P_2NN'$-Ph) were prepared according to their literature procedure.[33] NMR spectra were obtained at ambient temperature and pressure using a 400 MHz Varian MercuryPlus NMR spectrometer (400.00 MHz for ^{1}H, 161.98 MHz for ^{31}P, 128.4 MHz for ^{11}B, and 376.1 Hz for ^{19}F), an Agilent 500 MHz spectrometer with a OneNMR H/F{X} Probe (500 MHz for ^{1}H, 126 MHz for ^{13}C, 202 MHz for ^{31}P, and 160 MHz for ^{11}B), or an Agilent DD2-600 MHz spectrometer (600 MHz for ^{1}H, 151 MHz for ^{13}C, and 242 MHz for ^{31}P) unless stated otherwise. The ^{1}H and ^{13}C NMR were measured relative to partially deuterated solvent peaks. ^{31}P chemical shifts were measured relative to 85% phosphoric acid as an external reference. The elemental analyses were performed on a PerkinElmer 2400 CHN elemental analyzer. Solution magnetic susceptibilities were measured at 25 °C by a method originally described by Evans.[91] A solution of the compound in $CDCl_3$/cyclohexane (95/5 v/v) or CD_2Cl_2/cyclohexane (95/5 v/v) was prepared. The external standard consisted of a flame-sealed capillary containing $CDCl_3$/cyclohexane (95/5 v/v) or CD_2Cl_2/cyclohexane (95/5 v/v). The chemical shift difference of cyclohexane between the inset and the solution was used to determine the magnetic moment μ_{eff}.

2-(Diphenylphosphino)ethylamine (1). This compound was synthesized with a modified literature procedure.[68] In a Schlenk flask, diphenylphosphine (8.8 mL, 52 mmol) was dissolved in THF, and potassium *tert*-butoxide (11.6 g, 104 mmol) was added in portions giving rise to a bright orange solution. This was left to stir for 1 h. 2-Bromoethylamine hydrobromide (10.64 g, 52 mmol) was added to the mixture, and it was left to stir overnight at room temperature. The formation of a milky white solution was observed. The solvent was removed completely under a vacuum, and the resulting solid was stirred in pentane to remove leftover $HPPh_2$ and decanted. The product was triturated with ether and filtered through alumina, and the solvent was removed under a vacuum to give a yellow oil was used without further purification (3.97 g, 38%). ^{1}H NMR (400 MHz, $CDCl_3$): δ 7.43−7.30 (m, 10H), 2.84 (tt, J = 7.5 Hz, 9.4 Hz, 2H), 2.24 (t, J = 7.57 Hz, 2H), 1.67 (s,br, 2H). ^{31}P{^{1}H}NMR (162 MHz, $CDCl_3$): δ −21.85 (s).

N,N-bis(2-(Dicyclohexylphosphanyl)ethyl)-N-(2-(diphenylphosphanyl)ethyl)ethanamine (2)-NPP_2'-Cy. To a Schlenk flask was added **1** (500 mg, 2.18 mmol), cyclohexyl

https://dx.doi.org/10.1021/acs.inorgchem.0c01535
Inorg. Chem. XXXX, XXX, XXX−XXX

phosphonium dimer (1.4 g, 2.18 mmol), STAB (1.85 g, 8.73 mmol), 3 Å molecular sieves, and 25 mL of THF. The mixture was stirred overnight, and the resulting cloudy white solution was dried under a vacuum. The residue was extracted into 20 mL of DCM. The extract was washed air free on the Schlenk line with degassed NH_4Cl (3 × 15 mL) and degassed H_2O (3 × 15 mL). The organic layer was dried over Na_2SO_4 and then filtered through a short alumina plug. The solvent was removed under a vacuum to give a colorless oil was used without further purification (973 mg, 67%). ^{1}H NMR (400 MHz, $CDCl_3$): δ 7.45 (m, 4H), 7.37 (m, 6H), 1.84 (m, 6H), 1.72 (dt, J = 10.38, 19.80 Hz, 16H), 1.58 (t, J = 10.38 Hz, 4H), 1.31−1.20 (m, 16H), 1.17−1.11 (m, 8H), 0.88 (t, J = 7.33 Hz, 6H). ^{31}P{^{1}H} NMR (162 MHz, $CDCl_3$): δ −6.98 (s), −19.58 (s). MS-DART m/z calculated for $[C_{42}H_{67}NP_3]^+$: 678.4481. Found: 678.4484.

N,N-bis(2-(Diisopropylphosphanyl)ethyl)-N-(2-(diphenylphosphanyl)ethyl)ethanamine (3)-NPP$_2$′-^{i}Pr. The same general procedure was followed as in the synthesis of **2** but using the isopropyl-substituted phosphonium dimer. Colorless oil was used without further purification (733 mg, 84%). ^{1}H NMR (400 MHz, $CDCl_3$): δ 7.45−7.41 (m, 4H), 7.35−7.33 (m, 6H), 2.87, (s, br 4H), 1.84 (m, 2H), 1.72 (dq, 4H), 1.57 (s, br, 2H), 1.25−1.14 (m, 2H), 1.08−1.1 (m, 24H). ^{31}P{^{1}H} NMR (162 MHz, $CDCl_3$): δ 1.85 (s), −19.97 (s). MS-DART m/z calculated for $[C_{30}H_{51}NP_3]^+$: 518.3229. Found: 518.3232.

N,N-bis(2-(Diisobutylphosphanyl)ethyl)-N-(2-(diphenylphosphanyl)ethyl)ethanamine (4)-NPP$_2$′-^{i}Bu. The same general procedure was followed as in the synthesis of **2** but using the isobutyl-substituted phosphonium dimer. Colorless oil was used without further purification (838 mg, 68%). ^{1}H NMR (400 MHz, $CDCl_3$): δ 7.47−7.41 (m, 4H) 7.37−7.32 (m, 6H) 1.65 (septet, br, J = 6.43 Hz, 4H), 1.43−1.36 (m, 6H), 1.27 (d, J = 6.10 Hz, 8H), 0.98 (d, J = 6.43 Hz, 24H), 0.88 (m, 6H). ^{31}P{^{1}H} NMR (162 MHz, $CDCl_3$): δ −19.63 (s), −41.64 (s). MS-DART m/z calculated for $[C_{34}H_{59}NP_3]^+$: 574.3855. Found: 574.3853

N,N-bis(2-(Di-*o*-tolylphosphanyl)ethyl)-N-(2-(diphenylphosphanyl)ethyl)ethanamine (5)-NPP$_2$′-*o*Tol. The same general procedure was followed as in the synthesis of **2** but using the *o*-tolyl-substituted phosphonium dimer. Colorless oil was used without further purification (1.18 g, 76%). ^{1}H NMR (400 MHz, $CDCl_3$): δ 7.44−7.29 (m, 10H), 7.19−7.10 (m, 16H) 2.37 (s, 12H), 2.01 (t, J = 6.83 Hz, 4H), 1.84 (t, J = 7.26 Hz, 2H), 1.21 (t, J = 6.83 Hz, 4H), 0.88 (t, J = 7.26 Hz, 2H). ^{31}P{^{1}H} NMR (162 MHz, $CDCl_3$): δ −21.13 (s), −41.84 (s). MS-DART m/z calculated for $[C_{46}H_{51}NP_3]^+$: 710.3229. Found: 710.3231

N,N-bis(2-(Di-*p*-tolylphosphanyl)ethyl)-N-(2-(diphenylphosphanyl)ethyl)ethanamine (6)-NPP$_2$′-*p*Tol. The same general procedure was followed as in the synthesis of **2** but using the *p*-tolyl-substituted phosphonium dimer. A total of 100 mg of **2** was used and the other reagents were scaled down accordingly. Colorless oil was used without further purification (175 mg, 56%). ^{1}H NMR (300 MHz, CD_2Cl_2): δ 7.41−7.08 (m, 26H), 2.57−5.47 (m (br), 3H), 2.39−2.29 (m, 16H), 1.98−1.92 (m (br), 3H). ^{31}P{^{1}H} NMR (121 MHz, CD_2Cl_2): δ −20.06 (s), −26.33 (s). MS-DART m/z calculated for $[C_{46}H_{51}NP_3]^+$: 710.3229. Found: 710.3225

tris(2-(Diisobutylphosphaneyl)ethyl)amine (7)-NP$_3$. To a Schlenk flask was added ammonium acetate (0.308 g, 4 mmol), isobutyl phosphonium dimer (0.538 g, 1 mmol), STAB (0.848 g, 4 mmol), and THF (15 mL). The resulting mixture was stirred over 3 Å molecular sieves for 20 h and then filtered over Celite. One milliliter of MeOH was added to quench any residual borohydride, then the solvent was removed under a vacuum. The residue was extracted with pentane (15 mL) and then washed air free on the Schlenk line with degassed water (2 × 10 mL). The organic layer was dried over Na_2SO_4 and filtered and the solvent evaporated to give a colorless oil that was used without further purification (0.32 g, 91% with respect to phosphonium dimer). ^{1}H NMR (400 MHz, $CDCl_3$): δ 2.60 (m, 6H), 1.67 (m, 6H), 1.48 (m, 6H), 1.31 (m, 12H), 0.91 (d, J = 6.7 Hz, 36H). ^{31}P{^{1}H}NMR (162 MHz, $CDCl_3$): δ −41.6 (s). MS-DART m/z calculated for $[C_{30}H_{67}NP_3]^+$: 534.4481. Found: 534.4492

FeCl$_2$(P$_2$NN′-Cy) (8). A 20 mL vial was charged with $FeCl_2$ (30 mg, 0.237 mmol) and THF (6 mL) and stirred for 1 h at room temperature. P_2NN′-Cy (132 mg, 0.237 mmol) was dissolved in 1 mL of THF and added dropwise to the stirring $FeCl_2$ solution. A color change to orange was observed, and after continued stirring (∼2 h) a yellow solid began to precipitate out of solution. The vial was stirred overnight, then 8 mL of pentane was added and stirring continued for 3 h. The precipitated solid was collected on a filter frit, washed with additional pentane, and dried under a vacuum, giving a yellow solid (141 mg, 87%). Crystallization attempts via pentane diffusion into a saturated DCM solution always resulted in the formation of fibrous needles unsuitable for X-ray diffraction. Crystals suitable for X-ray diffraction were grown by layering a saturated MeOH solution with Et_2O. The complex is paramagnetic and ^{31}P NMR silent. ^{1}H NMR (500 MHz, $CDCl_3$): δ −21.66, −13.22, 12.19, 17.02, 42.82, 44.04, 47.23, 47.87, 49.66, 50.79, 78.04, 83.09, 138.58. Anal. calcd for $C_{34}H_{58}Cl_2FeN_2P_2$: C, 59.74; H, 8.55; N, 4.10. Found: C, 59.46; H, 8.44; N, 3.69. μ_{eff} (Evans method, $CDCl_3$) = 5.49 μ_B

[FeCl(P$_2$NN′-Cy)][BPh$_4$] (9). A 20 mL vial was charged with **8** (105 mg, 0.15 mmol) and MeOH (6 mL) to give a light yellow homogeneous solution. $NaBPh_4$ (61 mg, 0.18 mmol) was dissolved in 1 mL of MeOH and added dropwise. A light yellow solid immediately precipitated out of solution, and the mixture was stirred overnight. The solid was collected on a filter frit, washed with MeOH and pentane, and dried under a vacuum to give a pale yellow solid (100 mg, 69%). Crystals suitable for X-ray diffraction were grown by slow diffusion of pentane into a saturated DCM solution. The complex is paramagnetic and ^{31}P NMR silent. ^{1}H NMR (500 MHz, CD_2Cl_2): δ 85.81, 58.86, 52.53, 50.22, 33.28, 9.98, 8.68, 7.77, 7.38, 6.78, 4.48, 2.12, 1.14, 0.26, −0.41, −0.55, −0.68, −0.94, −1.34, −3.29, −4.67, −5.18, −6.58, −7.70, −10.85, −11.38, −17.43. Anal. calcd for $C_{58}H_{78}BClFeN_2P_2$: C, 72.02; H, 8.13; N, 2.90. Found: C, 72.33; H, 7.98; N, 2.83. τ_5 = 0.82. μ_{eff} (Evans method CD_2Cl_2) = 5.31 μ_B

[FeCl(P$_2$NN′-Cy)(CO)][BPh$_4$] (10). In a Schlenk flask, **9** (164 mg, 0.24 mmol) was dissolved in 15 mL of THF and reacted with a slow stream of carbon monoxide for 8 h. The color changed from yellow to light green and then to dark green. The solvent was removed under a vacuum, and the residue was dissolved in ethanol and precipitated by the addition of a solution of $NaBPh_4$ (85 mg, 0.25 mmol) in 5 mL of ethanol. The light yellow-green precipitate was collected on a filter frit, washed with benzene, and then dissolved in DCM and precipitated by the addition of Et_2O. The precipitate was collected on a filter frit and dried under a vacuum to give a light yellow-green solid (110 mg, 45%). Crystals suitable for X-ray diffraction were grown by slow evaporation of a DCM/Et_2O solution. ^{1}H NMR (400 MHz, DMSO-d_6): δ 8.32 (d, J = 5.9 Hz, 1H), 7.74 (t, J = 7.9 Hz, 1H), 7.24−7.18 (m, 10H), 6.92 (t, J = 7.4 Hz, 8H), 6.78 (t, J = 7.2 Hz, 4H), 4.84 (s, 2H), 2.30−1.11 (m, 48H), 0.63 (s (br), 4H). ^{31}P{^{1}H} NMR (162 MHz, DMSO-d_6): δ 66.5 (s). FT-IR (cm^{-1}): 1960 ν(CO). Anal. calcd for $C_{59}H_{78}BClFeN_2OP_2$: C, 71.19; H, 7.90; N, 2.81. Found: C, 71.22; H, 7.95; N, 2.74.

[Fe(H)(P$_2$NN′-Cy)(CO)][BPh$_4$] (11). To a solution of **10** (99 mg, 0.1 mmol) in 15 mL of THF was added dropwise a solution of $NaBH_4$ (56 mg, 1.5 mmol) in 3 mL of ethanol. The resulting ruby-red solution was stirred overnight and then filtered through Celite. The solvent was removed under a vacuum, and the product was dissolved in methanol and precipitated by the addition of a solution of $NaBPh_4$ (34 mg, 0.1 mmol) in minimal methanol. The precipitate was collected on a filter frit and then dissolved in benzene and filtered through Celite. The golden yellow solution was evaporated to give a yellow solid (53 mg, 56%). Crystals suitable for X-ray diffraction were grown by slow evaporation of a DCM/Et_2O solution. ^{1}H NMR (400 MHz, $CDCl_3$): δ 8.62 (d, J = 5.6 Hz, 1H), 7.48 (s (br), 8H), 7.35 (t, J = 7.4 Hz, 1H), 7.06−6.99 (m, 9H), 6.89 (t, J = 7.1 Hz, 4H), 6.40 (d, J = 7.9 Hz, 1H), 2.81 (s, 2H), 1.98−0.92 (m, 48H), −18.75 (t, $^2J_{HP}$ = 53.0 Hz, 1H). ^{31}P{^{1}H} NMR (162 MHz, $CDCl_3$): δ 82.5 (s). FT-IR (cm^{-1}): 1900 ν(CO). Anal. calcd for $C_{59}H_{79}BFeN_2OP_2$: C, 73.75; H, 8.28; N, 2.91. Found: C, 73.82; H, 8.31; N, 2.86.

[Fe(P$_2$NN′-Ph)(NCMe)$_2$][BPh$_4$]$_2$ (12). A 20 mL vial was charged with $FeCl_2$(P$_2$NN′-Ph) (74 mg, 0.11 mmol) and MeCN (10 mL) to

https://dx.doi.org/10.1021/acs.inorgchem.0c01535
Inorg. Chem. XXXX, XXX, XXX−XXX

give a yellow solution with suspended solids. $NaBPh_4$ (46 mg, 0.13 mmol) was dissolved in 1 mL of MeCN and added dropwise. The reaction mixture experienced a gradient color change to dark green which was short-lived, and then the color changed to orange-brown. The vial containing $NaBPh_4$ was then rinsed with an additional 1 mL of MeCN and added to the reaction mixture, and the vial was stirred overnight. The solution was then filtered through Celite to give a clear orange solution, which was dried under a vacuum and gave a dark orange oily film. The residue was triturated with EtOH to remove excess $NaBPh_4$ and a pink solid developed. The EtOH suspension was stirred overnight, and then the solid was collected on a filter frit, washed with EtOH and Et_2O, and dried under a vacuum to give a pink powder (90 mg, 82%). The pink solid redissolved in MeCN results in an orange solution. Crystals suitable for X-ray diffraction were grown by layering a saturated MeCN solution with Et_2O. ^1H NMR (500 MHz, CD_3CN): δ 2.53−2.58, (t (br), 2H (CH_2)), 2.79−2.85 (t (br), 2H (CH_2)), 2.97−3.08 (m, 2H (CH_2)), 3.29−3.34 (m, 2H (CH_2)), 3.81 (s, 2H (CH_2-py)), 6.43 (t, J = 6.7 Hz, 1H (Ar−$H_{pyridine}$)) [the remaining aromatic protons did not integrate properly even after acquiring a ^1H spectrum with 25 s relaxation delay], 6.83−6.86 (t, J = 7.2 Hz, Ar−H), 6.98−7.01 (t, J = 7.4 Hz, Ar−H), 7.21−7.36 (m, Ar−H), 7.56−7.59 (m, Ar−H), 7.82−7.85 (m, Ar−H). $^{31}P\{^1H\}$ NMR (202 MHz, CD_3CN): δ 56.44 (s). $^{11}B\{^1H\}$ NMR (160 MHz, CD_3CN): δ −6.61 (s). Anal. calcd for $C_{86}H_{80}B_2FeN_4P_2$: C, 78.91; H, 6.16; N, 4.28. Found: C, 79.22; H, 5.88; N, 3.91.

[Fe(H)(NPP_2'-^{i}Pr)(N_2)][BPh_4] (13). In a Schlenk flask, **3** (77 mg, 0.15 mmol), $FeCl_2$ (19 mg, 0.15 mmol), and $NaBPh_4$ (51 mg, 0.15 mmol) were dissolved in THF. The resulting mixture was stirred at room temperature overnight under argon, giving rise to a cloudy colorless solution, then filtered over Celite and dried under a vacuum. The resulting solid was dissolved in a minimal amount of DCM and then precipitated by addition to a rapidly stirring vial of Et_2O (10 mL). The precipitate was collected on a filter frit and dried under a vacuum, giving rise to a pale-yellow solid (80 mg). The full structural identity of the resulting solid was unable to be determined; however the complex was confirmed to be paramagnetic as it was ^{31}P NMR silent. The solid was used in the next step under an assumed structural identity without any additional purification or characterization. To a vial of the pale-yellow solid (102 mg, 0.11 mmol) under an argon atmosphere was added MeOH (8 mL), and the resulting slurry was placed in a cold well and cooled to −30 °C. $NaBH_4$ (25 mg, 0.66 mmol) was dissolved in a minimal amount of MeOH and added dropwise to the slurry, which immediately experienced a color change to orange and was left to stir overnight. The mixture was then transferred to a N_2 filled glovebox and dried fully under a vacuum. The residue was redissolved in benzene, resulting in a color change to yellow-green. The solution was then dried under a vacuum resulting in a yellow-green solid (65 mg, 64%). Crystals suitable for X-ray diffraction were grown over a period of four months by cooling a saturated benzene solution to −30 °C with occasional thawing for inspection. ^1H NMR (400 MHz, C_6D_6): δ 7.49 (t, J = 7.18 Hz, 4H), 7.35−7.30 (m, 6H), 2.87−2.69 (m, 4H), 1.60−1.51 (m, 6H) 1.34−1.28 (m, 6H), 1.06−1.02 (m, 24H), −9.30 (dt, J = 62.6, 44.6 Hz, 1H). $^{31}P\{^1H\}$ NMR (161.98 MHz, C_6D_6): δ 73.9 (d, J = 15 Hz), 46.7 (t, J = 15 Hz). FT-IR (cm^{-1}): 2080 $\nu(N_2)$, 1907 ν(Fe−H). Elemental analysis was attempted multiple times; however due to the high sensitivity of the complex, the results did not accurately reflect the X-ray confirmed structural identity.

[FeCl(NP_3)(CO)][BPh_4] (14). In a Schlenk flask, **7** (180 mg, 0.35 mmol) and $FeCl_2$ (44 mg, 0.35 mmol) were dissolved in 10 mL of THF under an argon atmosphere and stirred at 60 °C overnight giving rise to a beige solution. The flask was cooled to room temperature and then placed under a slow stream of carbon monoxide for 6 h. The solution immediately turned dark blue, and then gradually changed color to brown. The solution was evaporated under a vacuum, and the resulting brown solid was extracted with 3 mL of ethanol and precipitated by the addition of solid $NaBPh_4$ (0.120 g, 0.35 mmol). The precipitate was filtered, washed with MeOH, and dried under a vacuum, and then the resulting orange solids were dissolved in benzene, filtered over Celite, and dried under a vacuum to give an orange solid (265 mg, 78%). Crystals suitable for X-ray diffraction were grown by slow evaporation of a DCM/Et_2O solution. ^1H NMR (400 MHz, $CDCl_3$): δ 7.45 (s(br), 8H), 7.07 (t, J = 7.3 Hz, 8H), 6.93 (t, J = 7.1 Hz, 4H), 2.92−2.83 (m, 2H), 2.48−2.44 (m, 2H), 2.38−2.26 (m, 4H), 2.16−2.11 (m(br), 2H), 2.07−1.87 (m, 10H), 1.74−1.67 (m, 2H), 1.56−1.36 (m, 6H), 1.24−1.06 (m, 32H), 1.00 (d, J = 6.5 Hz, 6H). $^{31}P\{^1H\}$NMR (162 MHz, $CDCl_3$): δ 49.4 (d, J = 42.2 Hz), 69.8 (t, J = 42.5 Hz). FT-IR (cm^{-1}): 1940ν(CO). Anal. calcd for $C_{55}H_{86}BClFeNOP_3$: C, 67.94; H, 8.91; N, 1.44. Found: C, 67.96; H, 8.93; N, 1.39.

[Fe(H)(NP_3)(CO)][BPh_4] (15). To a solution of **14** (48 mg, 0.05 mmol) in 5 mL of THF was added a solution of $NaBH_4$(28 mg, 0.75 mmol) in 2 mL of ethanol, and the resulting solution was stirred overnight. The solution was evaporated under a vacuum, and the resulting yellow solid was extracted with 5 mL of benzene. The extract was filtered through Celite and evaporated to give a yellow solid (34 mg, 74%). Crystals suitable for X-ray diffraction were grown by slow evaporation of a DCM/Et_2O solution. ^1H NMR (400 MHz, $CDCl_3$): δ 7.41 (s (br), 8H), 7.06 (t, J = 6.9 Hz, 8H), 6.92 (t, J = 6.7 Hz, 4H), 2.21 (p, J = 6.1 Hz, 2H), 2.03 (d, J = 6.5 Hz, 4H), 2.00−1.86 (m, 6H), 1.75 (dd, J = 20.0, 11.4 Hz, 2H), 1.57 (dq, J = 24.6, 9.2, 8.0 Hz, 6H), 1.17−1.04 (m, 36H), −11.2 (dt, J = 68.1, 33.8 Hz, 1H). $^{31}P\{^1H\}$ NMR (162 MHz, $CDCl_3$): δ 63.6 (d, J = 20, Hz), 65.1 (t, J = 20 Hz). FT-IR (cm^{-1}): 1903 ν(CO). Anal. calcd for $C_{55}H_{87}BFeNOP_3$: C, 70.43; H, 9.35; N, 1.49. Found: C, 70.47; H, 9.38; N, 1.41.

Fe(NP_3)(CO) (16). To a solution of **15** (47 mg, 0.05 mmol) in 5 mL of THF was added solid KH (20 mg, 0.5 mmol), and the resulting mixture was stirred overnight. After filtration over Celite and evaporation of the solvent under a vacuum, the residue was extracted with 5 mL of benzene. The extract was filtered through Celite and evaporated to give a red solid (25 mg, 82%). Crystals suitable for X-ray diffraction were grown by slow evaporation of a benzene/hexane solution. ^1H NMR (400 MHz, C_6D_6): δ 2.78 (m, 1H), 2.43 (s(br), 4H), 1.83−1.62 (m, 20H), 1.38−1.23 (m, 5H), 1.17−1.05 (m, 36H). $^{31}P\{^1H\}$ NMR (162 MHz, C_6D_6): δ 64.05 (s). FT-IR (cm^{-1}): 1808 ν(CO). Anal. calcd for $C_{31}H_{66}FeNOP_3$: C, 60.28; H, 10.77; N, 2.26. Found: C, 60.31; H, 10.80; N, 2.21. τ_5 = 0.96.

■ ASSOCIATED CONTENT

Supporting Information

The Supporting Information is available free of charge at https://pubs.acs.org/doi/10.1021/acs.inorgchem.0c01535.

NMR spectra and IR spectra of CO compounds and crystallographic data tables (PDF)

Accession Codes

CCDC 2004808−2004816 contain the supplementary crystallographic data for this paper. These data can be obtained free of charge via www.ccdc.cam.ac.uk/data_request/cif, or by emailing data_request@ccdc.cam.ac.uk, or by contacting The Cambridge Crystallographic Data Centre, 12 Union Road, Cambridge CB2 1EZ, UK; fax: +44 1223 336033.

■ AUTHOR INFORMATION

Corresponding Author

Robert H. Morris − *Department of Chemistry, University of Toronto, Toronto, Ontario, Canada M5S 3H6;* orcid.org/0000-0002-7574-9388; Email: rmorris@chem.utoronto.ca

Authors

Matthew V. Gradiski − *Department of Chemistry, University of Toronto, Toronto, Ontario, Canada M5S 3H6;* orcid.org/0000-0001-7374-5554

Ali Nemati Kharat − *School of Chemistry, College of Science, University of Tehran, Tehran, Iran*

Maegan S. E. Ong − *Department of Chemistry, University of Toronto, Toronto, Ontario, Canada M5S 3H6*

https://dx.doi.org/10.1021/acs.inorgchem.0c01535
Inorg. Chem. XXXX, XXX, XXX−XXX

Alan J. Lough − *Department of Chemistry, University of Toronto, Toronto, Ontario, Canada M5S 3H6;* orcid.org/0000-0001-6012-0379

Samantha A. M. Smith − *Department of Chemistry, University of Toronto, Toronto, Ontario, Canada M5S 3H6;* orcid.org/0000-0003-0807-8315

Complete contact information is available at: https://pubs.acs.org/10.1021/acs.inorgchem.0c01535

Author Contributions

[§]These authors contributed equally.

Notes

The authors declare no competing financial interest.

■ ACKNOWLEDGMENTS

NSERC is acknowledged for a Discovery Grant to R.H.M. and the Strategic Grant "Catalytic Synthesis of Specialty Chemicals from Sustainable Resources." The Ontario Government is acknowledged for an Ontario Graduate Scholarship for M.V.G.

■ DEDICATION

This article is dedicated to the memory of Professor Deborah Zamble, a dear mentor and colleague and an extraordinary bioinorganic chemist.

■ REFERENCES

(1) Hewertson, W.; Watson, H. R. 283. The Preparation of Di- and Tri-Tertiary Phosphines. *J. Chem. Soc.* **1962**, 1490−1494.

(2) Suarez, T.; Fontal, B. Hydrogenation Reactions with $RuCl_2$(TRIPHOS). *J. Mol. Catal.* **1988**, *45*, 335−344.

(3) Ferretti, F.; Scharnagl, F. K.; Dall'Anese, A.; Jackstell, R.; Dastgir, S.; Beller, M. Additive-Free Cobalt-Catalysed Hydrogenation of Carbonates to Methanol and Alcohols. *Catal. Sci. Technol.* **2019**, *9*, 3548−3553.

(4) Walter, O.; Hüttner, G.; Kern, R. Preparation and Characterisation of $N(CH_2PPh_2)_3$,$N(CH_2PPh_2)_3Mo(CO)_3$ and $[HN(CH_2PPh_2)_3Mo(CO)_3]BF_4$. *Z. Naturforsch., B: J. Chem. Sci.* **1996**, *51*, 922−928.

(5) Apps, S. L.; White, A. J. P.; Miller, P. W.; Long, N. J. Synthesis and Reactivity of an N-Triphos Mo(0) Dinitrogen Complex. *Dalton Trans.* **2018**, *47*, 11386−11396.

(6) Phanopoulos, A.; Brown, N. J.; White, A. J. P.; Long, N. J.; Miller, P. W. Synthesis, Characterization, and Reactivity of Ruthenium Hydride Complexes of N-Centered Triphosphine Ligands. *Inorg. Chem.* **2014**, *53*, 3742−3752.

(7) Mani, F.; Sacconi, L. Five-Coordinate Chromium(II) Complexes with Nitrogen-Phosphorus Tetradentate Ligands. *Inorg. Chim. Acta* **1970**, *4*, 365−366.

(8) Sacconi, L.; Bertini, I. Low- and High-Spin Five-Coordinate Cobalt(II) and Nickel(II) Complexes with Tris(2-Diphenylphosphinoethyl)Amine. *J. Am. Chem. Soc.* **1968**, *90*, 5443−5446.

(9) Orioli, P. L.; Sacconi, L. Square Pyramidal Structure of a Five-Co-Ordinate Cobalt (II) Complex with the Tripod Ligand Tris-(2-Diphenylphosphinoethyl)Amine. *J. Chem. Soc. D* **1969**, 1012−1012.

(10) Sacconi, L.; Di Vaira, M.; Bianchi, A. Unusual Coordination in a Cobalt(II) Complex with the Tripod Ligand Tris(2-Diphenylphosphinoethyl)Amine. *J. Am. Chem. Soc.* **1970**, *92*, 4465−4466.

(11) Mealli, C.; Orioli, P. L.; Sacconi, L. Crystal and Molecular Structure of Di-Iodotris(2-Diphenylphosphinoethyl)Amine Cobalt-(II). *J. Chem. Soc. A* **1971**, 2691−2694.

(12) Sacconi, L.; Bertini, I. Five-Coordinate Nickel(II) Complexes with Nitrogen-Phosphorus and Nitrogen-Arsenic Tetradentate Ligands. *J. Am. Chem. Soc.* **1967**, *89*, 2235−2236.

(13) Bianchini, C.; Meli, A. Reactivity of Formaldehyde and Acetaldehyde Toward $[N(CH_2CH_2PPh_2)_3]Ni$ and $[N(CH_2CH_2PPh_2)_3]CoH$. *Organometallics* **1985**, *4*, 1537−1542.

(14) Bianchini, C.; Masi, D.; Meli, A.; Peruzzini, M.; Sabat, M.; Zanobini, F. Intra- and Intermolecular Activation of Sp2 Carbon-Hydrogen Bonds at Rhodium(I) and Iridium(I) Metal Centers. X-Ray Structure of the Cis σ-Cyclooctadienyl Hydride $[\{N(CH_2CH_2PPh_2)_3\}IrH(\sigma\text{-}C_8H_{11})]BPh_4\cdot CH_3COCH_3$. *Organometallics* **1986**, *5*, 2557−2559.

(15) Rossin, A.; Gutsul, E. I.; Belkova, N. V.; Epstein, L. M.; Gonsalvi, L.; Ledós, A.; Lyssenko, K. A.; Peruzzini, M.; Shubina, E. S.; Zanobini, F. Mechanistic Studies on the Interaction of $[(K^3\text{-}P,P,P\text{-}NP_3)IrH_3]$ $[NP_3 = N(CH_2CH_2PPh_2)_3]$ with HBF_4 and Fluorinated Alcohols by Combined NMR, IR, and DFT Techniques. *Inorg. Chem.* **2010**, *49*, 4343−4354.

(16) MacBeth, C. E.; Harkins, S. B.; Peters, J. C. Synthesis and Characterization of Cationic Iron Complexes Supported by the Neutral Ligands $NPi\text{-}Pr_3$, $NArPi\text{-}Pr_3$, and $NSt\text{-}Bu_3$. *Can. J. Chem.* **2005**, *83*, 332−340.

(17) Stoppioni, P.; Mani, F.; Sacconi, L. Halo-, Hydrido- and Dinitrogen-Complexes of Iron(II) with Tritertiary Phosphines. *Inorg. Chim. Acta* **1974**, *11*, 227−230.

(18) George, T. A.; Rose, D. J.; Chang, Y.; Chen, Q.; Zubieta, J. Reduction of Dinitrogen to Ammonia and Hydrazine in Iron(0) and Molybdenum(0) Complexes Containing the $N(CH_2CH_2PPh_2)_3$ Ligand. Crystal Structures of $[FeH(L)(N(CH_2CH_2PPh_2)_3)][BPh_4]$ ($L = N_2$, CO). *Inorg. Chem.* **1995**, *34*, 1295−1298.

(19) Mellone, I.; Peruzzini, M.; Rosi, L.; Mellmann, D.; Junge, H.; Beller, M.; Gonsalvi, L. Formic Acid Dehydrogenation Catalysed by Ruthenium Complexes Bearing the Tripodal Ligands Triphos and NP_3. *Dalton Trans.* **2013**, *42*, 2495−2501.

(20) Todisco, S.; Luconi, L.; Giambastiani, G.; Rossin, A.; Peruzzini, M.; Golub, I. E.; Filippov, O. A.; Belkova, N. V.; Shubina, E. S. Ammonia Borane Dehydrogenation Catalyzed by $(K^4\text{-}EP_3)Co(H)$ $[EP_3 = E(CH_2CH_2PPh_2)_3$; E = N, P] and H_2 Evolution from their Interaction with NH Acids. *Inorg. Chem.* **2017**, *56*, 4296−4307.

(21) Rossin, A.; Rossi, A.; Peruzzini, M.; Zanobini, F. Chemical Hydrogen Storage: Ammonia Borane Dehydrogenation Catalyzed by NP_3 Ruthenium Hydrides $(NP_3{=}N(CH_2CH_2PPh_2)_3)$. *ChemPlusChem* **2014**, *79*, 1316−1325.

(22) Joó, F. Breakthroughs in Hydrogen Storage—Formic Acid as a Sustainable Storage Material for Hydrogen. *ChemSusChem* **2008**, *1*, 805−808.

(23) Enthaler, S.; von Langermann, J.; Schmidt, T. Carbon Dioxide and Formic Acid—the Couple for Environmental-Friendly Hydrogen Storage? *Energy Environ. Sci.* **2010**, *3*, 1207−1217.

(24) Sordakis, K.; Tang, C.; Vogt, L. K.; Junge, H.; Dyson, P. J.; Beller, M.; Laurenczy, G. Homogeneous Catalysis for Sustainable Hydrogen Storage in Formic Acid and Alcohols. *Chem. Rev.* **2018**, *118*, 372−433.

(25) Schieweck, B. G.; Westhues, N. F.; Klankermayer, J. A Highly Active Non-Precious Transition Metal Catalyst for the Hydrogenation of Carbon Dioxide to Formates. *Chem. Sci.* **2019**, *10*, 6519−6523.

(26) Anaby, A.; Schelwies, M.; Schwaben, J.; Rominger, F.; Hashmi, A. S. K.; Schaub, T. Study of Precatalyst Degradation Leading to the Discovery of a New Ru(0) Precatalyst for Hydrogenation and Dehydrogenation. *Organometallics* **2018**, *37*, 2193−2201.

(27) Bautista, M. T.; Earl, K. A.; Maltby, P. A.; Morris, R. H. Stereochemical Control of the Exchange of Hydrogen Atoms Between Hydride and Dihydrogen Ligands in the Complexes $[M(\eta^2\text{-}H_2)(H)(Meso\text{- or Rac-Tetraphos-1})]^+$, M = Fe, Os. *J. Am. Chem. Soc.* **1988**, *110*, 4056−4057.

(28) Bautista, M. T.; Earl, K. A.; Maltby, P. A.; Morris, R. H.; Schweitzer, C. T. New Dihydrogen Complexes: The Synthesis and Spectroscopic Properties of Iron(II), Ruthenium(II), and Osmium-(II) Complexes Containing the Meso-Tetraphos-1 Ligand. *Can. J. Chem.* **1994**, *72*, 547−560.

(29) Prokopchuk, D. E.; Chambers, G. M.; Walter, E. D.; Mock, M. T.; Bullock, R. M. H_2 Binding, Splitting, and Net Hydrogen Atom

Transfer at a Paramagnetic Iron Complex. *J. Am. Chem. Soc.* **2019**, *141*, 1871−1876.
(30) Whited, M. T.; Rivard, E.; Peters, J. C. Complexes of Iron and Cobalt with New Tripodal Amido-Polyphosphine Hybrid Ligands. *Chem. Commun.* **2006**, 1613−1615.
(31) Deng, L.; Kang, B.; Englert, U.; Klankermayer, J.; Palkovits, R. Direct Hydrogenation of Biobased Carboxylic Acids Mediated by a Nitrogen-Centered Tridentate Phosphine Ligand. *ChemSusChem* **2016**, *9*, 177−180.
(32) Schnoor, A.-C.; Gradert, C.; Schleupner, M.; Krahmer, J.; Tuczek, F. Molybdenum Bis(Dinitrogen) Complexes Supported by NP_3 Ligands Containing Propylene Linkages: Symmetry Breaking and Geometrical Isomerism. *Z. Anorg. Allg. Chem.* **2015**, *641*, 83−90.
(33) Gradiski, M. V.; Tsui, B. T. H.; Lough, A. J.; Morris, R. H. PNN′ & P_2NN′ Ligands via Reductive Amination with Phosphine Aldehydes: Synthesis and Base-Metal Coordination Chemistry. *Dalton Trans.* **2019**, *48*, 2150−2159.
(34) Rautenstrauch, V.; Hoang-Cong, X.; Churlaud, R.; Abdur-Rashid, K.; Morris, R. H. Hydrogenation Versus Transfer Hydrogenation of Ketones: Two Established Ruthenium Systems Catalyze Both. *Chem. - Eur. J.* **2003**, *9*, 4954−4967.
(35) Sui-Seng, C.; Freutel, F.; Lough, A. J.; Morris, R. H. Highly Efficient Catalyst Systems Using Iron Complexes with a Tetradentate PNNP Ligand for the Asymmetric Hydrogenation of Polar Bonds. *Angew. Chem., Int. Ed.* **2008**, *47*, 940−943.
(36) Zuo, W.; Lough, A. J.; Li, Y. F.; Morris, R. H. Amine(Imine)-Diphosphine Iron Catalysts for Asymmetric Transfer Hydrogenation of Ketones and Imines. *Science* **2013**, *342*, 1080−1083.
(37) Demmans, K. Z.; Seo, C. S. G.; Lough, A. J.; Morris, R. H. From Imine to Amine: An Unexpected Left Turn. Cis-β Iron(II) PNNP′ Precatalysts for the Asymmetric Transfer Hydrogenation of Acetophenone. *Chem. Sci.* **2017**, *8*, 6531−6541.
(38) Mikhailine, A.; Lough, A. J.; Morris, R. H. Efficient Asymmetric Transfer Hydrogenation of Ketones Catalyzed by an Iron Complex Containing a P-N-N-P Tetradentate Ligand Formed by Template Synthesis. *J. Am. Chem. Soc.* **2009**, *131*, 1394−1395.
(39) Demmans, K. Z.; Olson, M. E.; Morris, R. H. Asymmetric Transfer Hydrogenation of Ketones with Well-Defined Manganese(I) PNN and PNNP Complexes. *Organometallics* **2018**, *37*, 4608−4618.
(40) Zuo, W.; Tauer, S.; Prokopchuk, D. E.; Morris, R. H. Iron Catalysts Containing Amine(Imine)Diphosphine P-NH-N-P Ligands Catalyze Both the Asymmetric Hydrogenation and Asymmetric Transfer Hydrogenation of Ketones. *Organometallics* **2014**, *33*, 5791−5801.
(41) Mikhailine, A. A.; Maishan, M. I.; Lough, A. J.; Morris, R. H. The Mechanism of Efficient Asymmetric Transfer Hydrogenation of Acetophenone Using an Iron(II) Complex Containing an (S,S)-$Ph_2PCH_2CH{=}NCHPhCHPhN{=}CHCH_2PPh_2$ Ligand: Partial Ligand Reduction Is the Key. *J. Am. Chem. Soc.* **2012**, *134*, 12266−12280.
(42) Sues, P. E.; Lough, A. J.; Morris, R. H. Stereoelectronic Factors in Iron Catalysis: Synthesis and Characterization of Aryl-Substituted Iron(II) Carbonyl P−N−N−P Complexes and Their Use in the Asymmetric Transfer Hydrogenation of Ketones. *Organometallics* **2011**, *30*, 4418−4431.
(43) Smith, S. A. M.; Morris, R. H. An Unsymmetrical Iron Catalyst for the Asymmetric Transfer Hydrogenation of Ketones. *Synthesis* **2015**, *47*, 1775−1779.
(44) Ranocchiari, M.; Mezzetti, A. PNNP Macrocycles: A New Class of Ligands for Asymmetric Catalysis. *Organometallics* **2009**, *28*, 1286−1288.
(45) Schotes, C.; Althaus, M.; Aardoom, R.; Mezzetti, A. Asymmetric Diels−Alder and Ficini Reactions with Alkylidene β-Ketoesters Catalyzed by Chiral Ruthenium PNNP Complexes: Mechanistic Insight. *J. Am. Chem. Soc.* **2012**, *134*, 1331−1343.
(46) Egloff, J.; Ranocchiari, M.; Schira, A.; Schotes, C.; Mezzetti, A. Highly Enantioselective Ruthenium/PNNP-Catalyzed Imine Aziridination: Evidence of Carbene Transfer from a Diazoester Complex. *Organometallics* **2013**, *32*, 4690−4701.
(47) Bigler, R.; Mezzetti, A. Isonitrile Iron(II) Complexes with Chiral N_2P_2 Macrocycles in the Enantioselective Transfer Hydrogenation of Ketones. *Org. Lett.* **2014**, *16*, 6460−6463.
(48) Bigler, R.; Otth, E.; Mezzetti, A. Chiral Macrocyclic N_2P_2 Ligands and Iron(II): A Marriage of Interest. *Organometallics* **2014**, *33*, 4086−4099.
(49) Bigler, R.; Huber, R.; Mezzetti, A. Highly Enantioselective Transfer Hydrogenation of Ketones with Chiral $(NH)_2P_2$ Macrocyclic Iron(II) Complexes. *Angew. Chem., Int. Ed.* **2015**, *54*, 5171−5174.
(50) Huber, R.; Bigler, R.; Mezzetti, A. Chiral Iron(II) NPPN Complexes: Synthesis and Application in the Asymmetric Strecker Reaction of Azomethine Imines. *Organometallics* **2015**, *34*, 3374−3384.
(51) Bigler, R.; Huber, R.; Stöckli, M.; Mezzetti, A. Iron(II)/$(NH)_2P_2$ Macrocycles: Modular, Highly Enantioselective Transfer Hydrogenation Catalysts. *ACS Catal.* **2016**, *6*, 6455−6464.
(52) Bigler, R.; Mezzetti, A. Highly Enantioselective Transfer Hydrogenation of Polar Double Bonds by Macrocyclic Iron(II)/$(NH)_2P_2$ Catalysts. *Org. Process Res. Dev.* **2016**, *20*, 253−261.
(53) Passera, A.; Mezzetti, A. The Manganese(I)-Catalyzed Asymmetric Transfer Hydrogenation of Ketones: Disclosing the Macrocyclic Privilege. *Angew. Chem., Int. Ed.* **2020**, *59*, 187−191.
(54) Lagaditis, P. O.; Sues, P. E.; Sonnenberg, J. F.; Wan, K. Y.; Lough, A. J.; Morris, R. H. Iron(II) Complexes Containing Unsymmetrical P−N−P′ Pincer Ligands for the Catalytic Asymmetric Hydrogenation of Ketones and Imines. *J. Am. Chem. Soc.* **2014**, *136*, 1367−1380.
(55) Smith, S. A. M.; Lagaditis, P. O.; Lüpke, A.; Lough, A. J.; Morris, R. H. Unsymmetrical Iron P-NH-P′ Catalysts for the Asymmetric Pressure Hydrogenation of Aryl Ketones. *Chem. - Eur. J.* **2017**, *23*, 7212−7216.
(56) Sonnenberg, J. F.; Lough, A. J.; Morris, R. H. Synthesis of Iron P-N-P′ and P-NH-P′ Asymmetric Hydrogenation Catalysts. *Organometallics* **2014**, *33*, 6452−6465.
(57) Lagaditis, P. O.; Mikhailine, A. A.; Lough, A. J.; Morris, R. H. Template Synthesis of Iron(II) Complexes Containing Tridentate P-N-S, P-N-P, P-N-N, and Tetradentate P-N-N-P Ligands. *Inorg. Chem.* **2010**, *49*, 1094−1102.
(58) Seo, C. S. G.; Tannoux, T.; Smith, S. A. M.; Lough, A. J.; Morris, R. H. Enantioselective Hydrogenation of Activated Aryl Imines Catalyzed by an Iron(II) P-NH-P′ Complex. *J. Org. Chem.* **2019**, *84*, 12040−12049.
(59) Sonnenberg, J. F.; Wan, K. Y.; Sues, P. E.; Morris, R. H. Ketone Asymmetric Hydrogenation Catalyzed by P-NH-P′ Pincer Iron Catalysts: An Experimental and Computational Study. *ACS Catal.* **2017**, *7*, 316−326.
(60) Abdur-Rashid, K.; Guo, R.; Lough, A. J.; Morris, R. H.; Song, D. Synthesis of Ruthenium Hydride Complexes Containing Beta-Aminophosphine Ligands Derived from Amino Acids and Their Use in the H_2-Hydrogenation of Ketones and Imines. *Adv. Synth. Catal.* **2005**, *347*, 571−579.
(61) Saudan, L. A.; Saudan, C. M.; Debieux, C.; Wyss, P. Dihydrogen Reduction of Carboxylic Esters to Alcohols under the Catalysis of Homogeneous Ruthenium Complexes: High Efficiency and Unprecedented Chemoselectivity. *Angew. Chem., Int. Ed.* **2007**, *46*, 7473−7476.
(62) van Putten, R.; Uslamin, E. A.; Garbe, M.; Liu, C.; Gonzalez-De-Castro, A.; Lutz, M.; Junge, K.; Hensen, E. J. M.; Beller, M.; Lefort, L.; Pidko, E. A. Non-Pincer-Type Manganese Complexes as Efficient Catalysts for the Hydrogenation of Esters. *Angew. Chem., Int. Ed.* **2017**, *56*, 7531−7534.
(63) Higuchi, T.; Tagawa, R.; Iimuro, A.; Akiyama, S.; Nagae, H.; Mashima, K. Tunable Ligand Effects on Ruthenium Catalyst Activity for Selectively Preparing Imines or Amides by Dehydrogenative Coupling Reactions of Alcohols and Amines. *Chem. - Eur. J.* **2017**, *23*, 12795−12804.
(64) Jackman, K. M. K.; Fogh, A. A.; Stubbs, J. M.; Blacquiere, J. M. Synthesis of Pd Phosphine-Imine Complexes and Their Reactivity with Base. *J. Organomet. Chem.* **2019**, *880*, 56−61.

https://dx.doi.org/10.1021/acs.inorgchem.0c01535
Inorg. Chem. XXXX, XXX, XXX−XXX

(65) Jiang, X.; Zhang, J.; Zhao, D.; Li, Y. Aldehyde Effect and Ligand Discovery in Ru-Catalyzed Dehydrogenative Cross-Coupling of Alcohols to Esters. *Chem. Commun.* **2019**, *55*, 2797−2800.
(66) Kim, Y.; Lee, J.; Son, Y.-H.; Choi, S.-U.; Alam, M.; Park, S. Novel Nickel(II), Palladium(II), and Platinum(II) Complexes Having a Pyrrolyl-Iminophosphine (PNN) Pincer: Synthesis, Crystal Structures, and Cytotoxic Activity. *J. Inorg. Biochem.* **2020**, *205*, 111015.
(67) Nasser, N.; Borecki, A.; Boyle, P. D.; Puddephatt, R. J. A Versatile Diphosphine Ligand: Cis and Trans Chelation or Bridging, with Self Association Through Hydrogen Bonding. *Inorg. Chem.* **2013**, *52*, 7051−7060.
(68) Pan, B.; Liu, B.; Yue, E.; Liu, Q.; Yang, X.; Wang, Z.; Sun, W.-H. A Ruthenium Catalyst with Unprecedented Effectiveness for the Coupling Cyclization of γ-Amino Alcohols and Secondary Alcohols. *ACS Catal.* **2016**, *6*, 1247−1253.
(69) Tan, X.; Wang, Y.; Liu, Y.; Wang, F.; Shi, L.; Lee, K.-H.; Lin, Z.; Lv, H.; Zhang, X. Highly Efficient Tetradentate Ruthenium Catalyst for Ester Reduction: Especially for Hydrogenation of Fatty Acid Esters. *Org. Lett.* **2015**, *17*, 454−457.
(70) Xu, W.; Langer, R. Probing the Effect of Heterocycle-Bonding in PNX-Type Ruthenium Pre-Catalysts for Reactions Involving H_2. *Dalton Trans.* **2015**, *44*, 16785−16790.
(71) Takeshita, T.; Nakajima, Y. Deprotonation of a PNNP-Iron Complex: Expanding the Concept of Metal-Ligand Cooperation to the PNNP-Iron System. *Chem. Lett.* **2019**, *48*, 364−366.
(72) Kato, T.; Kuriyama, S.; Nakajima, K.; Nishibayashi, Y. Catalytic C-H Borylation Using Iron Complexes Bearing 4,5,6,7-Tetrahydroisoindol-2-Ide-Based PNP-Type Pincer Ligand. *Chem. - Asian J.* **2019**, *14*, 2097−2101.
(73) Holland, A. M.; Oliver, A. G.; Iluc, V. M. Iron Pyrrole-Based PNP Pincer Ligand Complexes as Catalyst Precursors. *Acta Crystallogr., Sect. C: Struct. Chem.* **2017**, *73*, 569−574.
(74) Thompson, C. V.; Arman, H. D.; Tonzetich, Z. J. A Pyrrole-Based Pincer Ligand Permits Access to Three Oxidation States of Iron in Organometallic Complexes. *Organometallics* **2017**, *36*, 1795−1802.
(75) Buchard, A.; Heuclin, H.; Auffrant, A.; Le Goff, X. F.; Le Floch, P. Coordination of Tetradentate X_2N_2 (X = P, S, O) Ligands to Iron(II) Metal Center and Catalytic Application in the Transfer Hydrogenation of Ketones. *Dalton Trans.* **2009**, 1659−1667.
(76) Jia, G.; Drouin, S. D.; Jessop, P. G.; Lough, A. J.; Morris, R. H. Use of the New Ligand $P(CH_2CH_2PCy_2)_3$ in the Synthesis of Dihydrogen Complexes of Iron(II) and Ruthenium(II). *Organometallics* **1993**, *12*, 906−916.
(77) Field, L. D.; Guest, R. W.; Vuong, K. Q.; Dalgarno, S. J.; Jensen, P. Iron(0) and Ruthenium(0) Complexes of Dinitrogen. *Inorg. Chem.* **2009**, *48*, 2246−2253.
(78) Lagaditis, P. O.; Sues, P. E.; Lough, A. J.; Morris, R. H. Exploring the Decomposition Pathways of Iron Asymmetric Transfer Hydrogenation Catalysts. *Dalton Trans.* **2015**, *44*, 12119−12127.
(79) Lagaditis, P. O.; Lough, A. J.; Morris, R. H. Low-Valent Ene−Amido Iron Complexes for the Asymmetric Transfer Hydrogenation of Acetophenone without Base. *J. Am. Chem. Soc.* **2011**, *133*, 9662−9665.
(80) Zuo, W.; Prokopchuk, D. E.; Lough, A. J.; Morris, R. H. Details of the Mechanism of the Asymmetric Transfer Hydrogenation of Acetophenone Using the Amine(Imine)Diphosphine Iron Precatalyst: The Base Effect and The Enantiodetermining Step. *ACS Catal.* **2016**, *6*, 301−314.
(81) Jayarathne, U.; Zhang, Y.; Hazari, N.; Bernskoetter, W. H. Selective Iron-Catalyzed Deaminative Hydrogenation of Amides. *Organometallics* **2017**, *36*, 409−416.
(82) Rivada-Wheelaghan, O.; Dauth, A.; Leitus, G.; Diskin-Posner, Y.; Milstein, D. Synthesis and Reactivity of Iron Complexes with a New Pyrazine-Based Pincer Ligand, and Application in Catalytic Low-Pressure Hydrogenation of Carbon Dioxide. *Inorg. Chem.* **2015**, *54*, 4526−4538.
(83) Gorgas, N.; Stöger, B.; Veiros, L. F.; Pittenauer, E.; Allmaier, G.; Kirchner, K. Efficient Hydrogenation of Ketones and Aldehydes Catalyzed by Well-Defined Iron(II) PNP Pincer Complexes: Evidence for an Insertion Mechanism. *Organometallics* **2014**, *33*, 6905−6914.
(84) Mazza, S.; Scopelliti, R.; Hu, X. Chemoselective Hydrogenation and Transfer Hydrogenation of Aldehydes Catalyzed by Iron(II) PONOP Pincer Complexes. *Organometallics* **2015**, *34*, 1538−1545.
(85) Langer, R.; Diskin-Posner, Y.; Leitus, G.; Shimon, L. J. W.; Ben-David, Y.; Milstein, D. Low-Pressure Hydrogenation of Carbon Dioxide Catalyzed by an Iron Pincer Complex Exhibiting Noble Metal Activity. *Angew. Chem., Int. Ed.* **2011**, *50*, 9948−9952.
(86) Morris, R. H. Estimating the Wavenumber of Terminal Metal-Hydride Stretching Vibrations of Octahedral d^6 Transition Metal Complexes. *Inorg. Chem.* **2018**, *57*, 13809−13821.
(87) Morris, R. H. Estimating the Acidity of Transition Metal Hydride and Dihydrogen Complexes by Adding Ligand Acidity Constants. *J. Am. Chem. Soc.* **2014**, *136*, 1948−1959.
(88) Sung, M. M. H.; Morris, R. H. Density Functional Theory Calculations Support the Additive Nature of Ligand Contributions to the pK_a of Iron Hydride Phosphine Carbonyl Complexes. *Inorg. Chem.* **2016**, *55*, 9596−9601.
(89) Field, L. D.; Messerle, B. A.; Smernik, R. J. Synthesis and Properties of Iron(II) Hydride Complexes Containing the Tripodal Tetraphosphine Ligand $P(CH_2CH_2PMe_2)_3$. *Inorg. Chem.* **1997**, *36*, 5984−5990.
(90) Mikhailine, A. A.; Lagaditis, P. O.; Sues, P. E.; Lough, A. J.; Morris, R. H. New Cyclic Phosphonium Salts Derived from the Reaction of Phosphine-Aldehydes with Acid. *J. Organomet. Chem.* **2010**, *695*, 1824−1830.
(91) Evans, D. F. The Determination of the Paramagnetic Susceptibility of Substances in Solution by Nuclear Magnetic Resonance. *J. Chem. Soc.* **1959**, 2003−2005.

https://dx.doi.org/10.1021/acs.inorgchem.0c01535
Inorg. Chem. XXXX, XXX, XXX−XXX